The Influence of Texture on the Magnetoelastic Properties of Polycrystalline TbDy Alloys

Thesis by

Nathan R. Good

In Partial Fulfillment of the Requirements
for the Degree of
Doctor of Philosophy

California Institute of Technology
Pasadena, California

2001
(Submitted May 24, 2001)

To my parents and my brother.

Acknowledgements

First, I wish to thank my advisor, Professor Brent Fultz, for his patient support of me and my research during the last four years. His willingness to listen to my concerns and provide guidance in and out of the lab at seemingly any time proved to be endlessly helpful, while his relaxed enthusiasm for science fostered a work environment full of creativity and enjoyment. The efforts of Dr. Jennifer Dooley and Jason Graetz form a large part of the work in this thesis, and I am grateful for their insights and encouragement as well as their contributions to my research. My good friends and fellow students Dr. Ashish Bhardwaj, Dr. Michael Manley, Ann Lee, and Dane Boysen provided both useful scientific insights as well as entertaining and meaningful experiences away from the lab. The willingness of my colleagues and fellow students, particularly Dr. Channing Ahn, Jiao Lin, Alan Yue, Dr. Paul Kim and Dr. Art Clark, to lend their assistance whenever possible never ceased to amaze me and for this I am indebted to them. Finally, the love and support of my parents Ray and Win and my brother Stephen has been the foundation of my strength and desire to achieve this and every other goal in my life..

Abstract

An investigation into the influence of texture on the magnetoelastic properties of cold-rolled polycrystalline terbium-dysprosium alloys has been performed. Significant influence of grain orientations on the thermal expansion, magnetostrictive and magnetomechanical damping properties of TbDy were observed.

Drop cast ingots of TbDy alloys were deformed by cold-rolling and annealing with the aim of reorienting grains for large magnetostrictive strains and damping capacities. Thermal expansion coefficients of single crystal and polycrystalline samples of TbDy were measured from 77 - 570 K. These measurements confirmed the expected strong reorientation of the c-axes of grains toward the direction of applied force during deformation. The anisotropy of thermal expansion between the rolling and applied stress directions provided a measure of the effectiveness of various sample preparations for maximizing magnetocrystalline anisotropy. Furthermore, the effects of magnetic phase transitions on thermal expansion through the Curie and Neel points of TbDy revealed thermal expansion anisotropy between grain orientations in the rolling and transverse directions of deformation.

Magnetostrictive strains along the rolling direction of polycrystalline TbDy alloys were measured at 77 K. Saturation magnetostriction of up to 55% of previous single crystal results were observed. Minimal applied stress was required to obtain near maximum magnetostrictions for all of the samples tested. This suggests a preloading mechanism within the grain structure of polycrystalline TbDy not present in single crystals. Also in contrast with single crystal measurements, the performance of more economical commercial purity (99.7%) samples was seen to be somewhat higher than similarly prepared high

purity (99.94%) samples. Resistance to deterioration of performance over multiple cycles was observed, as changes in magnetostriction over 150 cycles at 0.1 Hz were within measurement errors. By comparing thermal expansion anisotropy of TbDy samples with peak magnetostrictive strain, a clear proportionality between texture and magnetostrictive performance was established. Deviations from this pattern by samples with more deformation and annealing suggest microstructural mechanisms beyond average grain orientation impacting magnetostriction.

Magnetomechanical damping effects were observed for polycrystalline TbDy samples through compression stress-strain curves. Elastic moduli at 77 K was measured to be up to 80% less than at 300 K, with a large hysteresis present in the stress-strain curves of all samples tested below the Curie point. Damping capacity was measured as the stress-strain hysteresis loop divided by the total area under the stress-strain curve. Damping capacities up to 23% were measured for polycrystalline TbDy alloys. Larger magnetomechanical damping was observed at lower strains, with higher strains corresponded to saturation of magnetic domain realignment, smaller damping capacities and larger elastic moduli. Samples with larger magnetostrictions displayed larger damping capacities over a wide range of applied stresses, and also had consistently lower elastic moduli at 77K.

Mechanisms of damping were investigated by fitting magnetostriction, elastic modulus and estimated strain of damping saturation of TbDy alloys to a model of magnetomechanical energy dissipation. This model relates magnetomechanical damping to magnetic hysteresis, neglecting microstructural influences not present in magnetostriction data. The damping capacities predicted by this model were approximately an order of magnitude

higher than experimental results. This result suggests a prominent role of microstructural interactions in the domain realignments responsible for magnetoelastic damping.

Contents

List of Figures

List of Tables

Chapter 1

Mechanisms of Magnetostriction

1.1 Microscopic Theory of Magnetostriction

Magnetostriction is the property exhibited by all ferromagnetic materials whereby a change in shape of the material results from magnetization. The origin of magnetostrictive strain lies in the interaction between three properties of a ferromagnetic material. The first of these, the magnetic anisotropy energy, dictates the energy cost of changing the direction of magnetization of the material. The exchange interactions between electron spins, dipoles, quadrupoles and higher order terms, and the elastic energy of the material under stress are coupled to the anisotropy to create magnetostriction. The first two of these properties are magnetic in nature and are described in general by the interaction of magnetic dipole moments. In general, the arrangements of orbital and spin angular momenta of electrons are the source of atomic magnetic dipole moments of atoms. Hund's rules govern the arrangement of these angular momentum vectors. The first two rules specify that, subject to the exclusion principle, spin and orbital angular momenta are maximized so

as to minimize Coulombic potential energy. In addition, a third rule governs the summation of the orbital and spin angular momenta as a function of the number of electrons in a shell. This requirement arises from the spin-orbit interaction:

$$w_{\mathrm{SO}} = \lambda \mathbf{L} \cdot \mathbf{S} \tag{1.1}$$

In the case of atoms with unpaired electron spins, this is nonzero and subjects the unpaired electron to a torque from the magnetic field of the nucleus. If a shell is more than half-filled, only negative-spin electrons contribute to the orbital angular momentum. The resultant parallelism between $\mathbf{L}$ and $\mathbf{S}$ lead to the total angular momentum $\mathbf{J} = \mathbf{L} + \mathbf{S}$, i.e., $w_{\mathrm{SO}} < 0$. Conversely, for a shell filled halfway or less, $\mathbf{J} = \mathbf{L} - \mathbf{S}$, $w_{\mathrm{SO}} > 0$. These rules are essential in determining the magnetic dipole moment of an atom:

$$\boldsymbol{\mu} = -g\mu_{\mathrm{B}}\mathbf{J},\ g = 1 + \frac{J(J+1) + S(S+1) - L(L+1)}{2J(J+1)} \tag{1.2}$$

Once the dipole moments of the atoms have been determined, their interaction energies can be computed using the equation:

$$w(r, \cos\theta) = g(r) + l(r)\left(\cos^2\theta - \frac{1}{3}\right) + q(r)\left(\cos^4\theta - \frac{6}{7}\cos^2\theta + \frac{3}{35}\right) + \ldots \tag{1.3}$$

with r as the lattice constant and θ the angle between the bond and the magnetic moments. The exchange interaction between spins, $g(r)$, is independent of magnetization direction and hence does not contribute to length magnetostriction, which is magnetoelastic expansion along specific axes and the phenomena of interest to this investigation. (However, $g(r)$ does contribute to volume magnetostriction, an isotropic volume expansion of a magnetized

material). The dominant term in length magnetostriction is the dipole-dipole interaction $l(r)\left(\cos^2\theta - 1/3\right)$, while the quadrupole and higher order terms are generally negligible [1]. If we express the pair energy in terms of direction cosines of domain magnetization $(\alpha_1, \alpha_2, \alpha_3)$ and of the bond direction $(\beta_1, \beta_2, \beta_3)$, we obtain:

$$w(r,\theta) = l(r)\left\{(\alpha_1\beta_1 + \alpha_2\beta_2 + \alpha_3\beta_3)^2 - \frac{1}{3}\right\} \tag{1.4}$$

If we distort the crystal such that $r \rightarrow r'$, $\beta \rightarrow \beta'$, then we have [2]

$$\beta_k' = c\left(\beta_k + \varepsilon_{km}\beta_m + u_k\right),\ r' = r/c \tag{1.5}$$

$$c = 1 - \left(\beta_k\varepsilon_{km}\beta_m + \beta_k u_k\right) \tag{1.6}$$

Eq. 1.6 is a normalization factor to second order in ε and u, the deformation tensor and relative atomic displacements in the unit cell. We can then find the change in w to an equivalent order of approximation as follows: first, we find the change in bond strength under deformation,

$$l(r') = l(r) + (1-c)\frac{\partial l}{\partial r} \tag{1.7}$$

The above equations 1.4-1.7 can then be combined to yield the change in w due lattice deformation:

$$\delta w_{\text{ud}} = 2l\sum(\alpha\cdot\beta)\left[\alpha\cdot\varepsilon\cdot\beta - (\alpha\cdot\beta)\,\beta\cdot\varepsilon\cdot\beta\right] + r\frac{\partial l}{\partial r}\sum\beta\cdot\varepsilon\cdot\beta\left[(\alpha\cdot\beta)^2 - \frac{1}{3}\right] \tag{1.8}$$

$$\delta w_{\text{int}} = -\left(2l - r\frac{\partial l}{\partial r}\right)\sum u\cdot\beta\,(\alpha\cdot\beta)^2 \tag{1.9}$$

Equation 1.8 refers to the change in w due to uniform deformation, while 1.9 refers to the effects of internal distortions. By performing the above summations and minimizing the resultant energy densities with respect to the lattice strains, saturation magnetoelastic strains are determined.

Further analysis of magnetostrictive deformation of a particular material requires knowledge of its crystal structure. The case of interest in this investigation is the hexagonal structure of terbium and dysprosium. In the hexagonal case, performing the above summations and dividing by crystal volume yields [2,3]

$$\begin{aligned} U_{\mathrm{ME}} &= B_1^{\alpha,2}\left(\varepsilon_{11}+\varepsilon_{22}\right)\left(\alpha_3^2-\frac{1}{3}\right)+B_2^{\alpha,2}\varepsilon_{33}\left(\alpha_3^2-\frac{1}{3}\right) \\ &\quad +B^{\gamma,2}\left[\frac{1}{2}\left(\varepsilon_{11}-\varepsilon_{22}\right)\left(\alpha_1^2-\alpha_2^2\right)+\varepsilon_{12}\alpha_1\alpha_2\right] \\ &\quad +B^{\varepsilon,2}\left(\varepsilon_{13}\alpha_1\alpha_3+\varepsilon_{23}\alpha_2\alpha_3\right)+B_{\mathrm{int}}^{\gamma}\left[\frac{u_2}{2}\left(\alpha_1^2-\alpha_2^2\right)\right)+u_1\alpha_1\alpha_2\Big] \end{aligned} \tag{1.10}$$

$$B_1^{\alpha} = -\frac{N}{2}\left(2l+r\frac{\partial l}{\partial r}\right) \tag{1.11}$$

$$B_2^{\alpha} = N\left(2l+r\frac{\partial l}{\partial r}\right) \tag{1.12}$$

$$B^{\gamma,2} = N\left(\frac{7}{3}l+\frac{5}{6}r\frac{\partial l}{\partial r}\right) \tag{1.13}$$

$$B_{\mathrm{int}}^{\gamma,2} = \frac{\sqrt{3}}{6}\left(2l-r\frac{\partial l}{\partial r}\right) \tag{1.14}$$

$$B^{\varepsilon,2} = \frac{4}{3}N\left(4l+r\frac{\partial l}{\partial r}\right) \tag{1.15}$$

These magnetoelastic coefficients can be related to saturation strains of magnetostriction by minimizing the total energy. If we exclude the effects of internal orthorhombic

distortions, we obtain the following:

$$\lambda_1^\alpha = \lambda_a^c - \frac{1}{2}\lambda_a^a - \frac{1}{2}\lambda_a^b = -\frac{B_1^\alpha\left(c_{33}+2c_{13}\right)}{c_{11}c_{33}+c_{12}c_{33}-2c_{13}^2} \tag{1.16}$$

$$\lambda_2^\alpha = \lambda_c^c - \lambda_c^a = -\frac{B_2^\alpha\left(c_{11}+c_{12}+c_{13}\right)}{c_{11}c_{33}+c_{12}c_{33}-2c_{13}^2} \tag{1.17}$$

$$\lambda^{\gamma,2} = \lambda_a^a - \lambda_a^b = -\frac{B^{\gamma,2}}{c_{11}-c_{12}} \tag{1.18}$$

$$\lambda^{\varepsilon,2} = \lambda_e^e - \lambda_e^f = -2\frac{B^{\varepsilon,2}}{c_{44}} \tag{1.19}$$

with λ_j^i being the magnetostriction of the j-axis under a field applied in the i-axis direction (e and f being the $\left[1/\sqrt{2},0,1/\sqrt{2}\right]$ and $\left[1/\sqrt{2},0,-1/\sqrt{2}\right]$ directions). The elastic stiffness coefficients c_{ij} are exclusive of magnetoelastic effects, i.e., they are measured above the Curie point. The result can be further simplified in the case of magnetization confined within the basal plane (as we assume for terbium-dysprosium (TbDy) alloys), generally eliminating magnetostriction terms outside the basal plane a and b directions. In our investigation, the quantity of interest is the length magnetostriction $\lambda^{\gamma,2}$ which is a measure of the change in length along an axis of magnetization in the basal plane for a hexagonal material.

Although this model allows for a determination of magnetostrictive constants from the fundamental pair interactions of magnetic dipoles, its power is largely constrained by difficulties in measuring internal orthorhombic strains [2]. For materials of high magnetic anisotropy, most terms are small compared to the length magnetostriction $\lambda^{\gamma,2}$ in any case. While this model is useful in studying materials with more subtle magnetoelastic properties such as Co, a more direct approach is commonly used to characterize highly anisotropic magnetoelastic materials.

1.2 Macroscopic Approach

A simpler characterization of magnetostrictive behavior of single crystals can be found using the thermodynamic enthalpy of a crystal in terms of elastic compliances, stresses, magnetostriction and anisotropy constants and magnetization components along orthogonal axes [4]. While the computations involved are complex in the hexagonal case and the general result is lengthy, considerable simplification can be made for a material with high magnetoelastic anisotropy. Generally, magnetostriction of hexagonal crystals is described in terms of direction cosines of magnetostriction β_1,β_2,β_3 and direction cosines of magnetization $\alpha_1,\alpha_2,\alpha_3$ by the following equation [5]:

$$\begin{aligned}
\Delta l/l &= A\left[2\alpha_1\alpha_2\beta_1 + \left(\alpha_1^2 - \alpha_2^2\right)\beta_2\right]^2 \\
&\quad + B\alpha_3^2\left[(\alpha_1\beta_1 + \alpha_2\beta_2)^2 - (\alpha_1\beta_2 - \alpha_2\beta_1)^2\right] \\
&\quad + C\left[(\alpha_1\beta_1 + \alpha_2\beta_2)^2 - (\alpha_1\beta_2 - \alpha_2\beta_1)^2\right] \\
&\quad + D\left(1 - \alpha_3^2\right)\left(1 - \beta_3^2\right) + E\alpha_3^2\beta_3^2\left(1 - \alpha_3^2\right) \\
&\quad + F\alpha_3^2\left(1 - \alpha_3^2\right) + G\beta_3^2\left(1 - \alpha_3^2\right) + H\alpha_3\beta_3\left(\alpha_1\beta_1 + \alpha_2\beta_2\right) \\
&\quad + I\alpha_3^2\beta_3\left(\alpha_1\beta_1 + \alpha_2\beta_2\right) + J\alpha_3^2\left(1 - \beta_3^2\right) + K\alpha_3^2\beta_3^2
\end{aligned} \tag{1.20}$$

This equation can be simplified by considering the high magnetic anisotropy of the c-axis in TbDy, resulting in the need for excessively high fields for rotation of the magnetization out of the basal plane. Therefore, we assume $\alpha_3 = 0$ and we obtain

$$\Delta l/l = A\left[2\alpha_1\alpha_2\beta_1 + \left(\alpha_1^2 - \alpha_2^2\right)\beta_2\right]^2 +$$

$$C\left[(\alpha_1\beta_1+\alpha_2\beta_2)^2-(\alpha_1\beta_2-\alpha_2\beta_1)^2\right]+ \tag{1.21}$$
$$D\left(1-\beta_3^2\right)+G\beta_3^2$$

Further simplification can be made by considering a reference to the strain of the crystal when the magnetization is along the a-axis (i.e., setting $\alpha_1 = 1$, $\alpha_2 = 0$). By doing this, we can find the strain difference between this reference state and any other state magnetization in the basal plane. The a-axis magnetostriction of a hexagonal crystal with a hard c-axis can then be described as follows: with ϕ as the angle of rotation of the magnetization in the basal plane (i.e., $\alpha_1 = \cos\phi$, $\alpha_2 = \sin\phi$), the a-axis magnetostriction is [5]

$$\Delta l/l = A\sin^2 2\phi + 2C\sin^2\phi \tag{1.22}$$

The constants A and C are second- and fourth-order basal plane magnetostriction constants and are typically the fundamental magnetostriction constants measured for hard c-axis hexagonal crystals. In the case of TbDy alloys, the second-order magnetostriction constant is approximately one order of magnitude higher than the fourth-order constant for Tb_xDy_{1-x}, $0.6 \leq x \leq 0.76$ [6].

1.3 Magnetocrystalline Anisotropy

In addition to the magnetostriction coefficients, magnetocrystalline anisotropy is central in characterizing strain induced by a magnetic field. In general, ferromagnetic alloys have a preferred direction of spontaneous magnetization which corresponds with a minima of internal energy. This arises from spin-orbit interactions of electrons which tend to distort

their orbits from spherical to lower symmetries dependent on spin direction. Therefore, spin direction rotation induced by magnetization alters exchange and electrostatic energies between atoms. The result is an energy dependence on the direction of magnetization. This magnetocrystalline anisotropy is tied to the crystal structure and generally shares its symmetry. For hexagonal crystals, magnetocrystalline anisotropy has been shown to be [7]

$$H_K = K_2 P_2(\cos\theta) + K_4 P_4(\cos\theta) + K_6 P_6(\cos\theta) + K_6^6 \sin^6\theta \cos 6\phi \qquad (1.23)$$

P_n are Legendre polynomials and θ and ϕ are measured with respect to the c- and a-axes, respectively. The K_2 term dominates the uniaxial anisotropy the K_6^6 term dominates anisotropy in the basal plane. Generally, large differences in magnetocrystalline anisotropy for different crystal directions confine the magnetization to "easy directions," i.e., directions of low anisotropy. Since anisotropy is very dependent on the structure of orbital magnetic moments of atoms in a crystal, ferromagnetic elements of similar crystal structure can have widely different anisotropy properties. For example, hcp Co has an "easy c-axis" with $K_2 = 4.3 \times 10^6$ erg/cm^3 at room temperature. Therefore, there is an energy cost for rotating the vector of magnetization away from the c-axis [8]. In contrast is the case of Tb and Dy, measured values of K_2 and K_6^6 for which are given in Table 1.1. There are two important aspects of the magnetostrictive properties of TbDy arising from the magnetocrystalline anisotropy of Tb and Dy. First, the values of K_2 are positive and 2-3 orders of magnitude greater than K_6^6 for both elements [7]. The particularly huge anisotropy in the c-axis of Tb and Dy, shared by other rare earth elements as well, arises from orbital magnetic moments confined to the inner $4f$ electron shell and therefore unquenched by the

crystal fields. This results in a magnetization always in the basal plane unless a large field is applied along the c-axis to overcome the large energy penalty for magnetization in this direction - the term for this property is a "hard c-axis." Secondly, the opposite signs of K_6^6 for Tb and Dy allow for compositions of Tb_xDy_{1-x} which can result in a vanishingly small basal plane anisotropy. In fact, due to small changes in the anisotropy itself arising from magnetostriction, the value of K_6^6 cannot be kept at zero, but very small values of this constant result in a situation where the magnetization can be rotated in the basal plane with little energy penalty arising from anisotropy. By changing the composition of Tb and Dy in an alloy, one can then optimize magnetocrystalline anisotropy for a given application (most commonly, minimization at a specific temperature). Since K_6^6 is temperature dependent, the ideal composition for minimum anisotropy of a Tb_xDy_{1-x} is also temperature dependent, with $x = 0.6$ at 77 K for example [7].

Element	K_2 (erg/cm^3)	K_6^6 (erg/cm^3)
Tb	5.5×10^8 @ 11 K	2.4×10^6 @ 4 K
	1.7×10^8 @ 205 K	2.0×10^5 @ 140 K
Dy	5.0×10^8 @ 22 K	-7.5×10^6 @ 4 K
	1.7×10^8 @ 152 K	-2.0×10^6@ 120 K

Table 1.1: Magnetic anisotropy constants for single crystal Tb and Dy

The particularly huge anisotropy in the c-axis of Tb and Dy, shared by other hcp rare earth elements as well, arises from orbital magnetic moments confined to the inner $4f$ electron shell and therefore unquenched by the crystal fields. In the case of Tb, the orbital moment of the $4f$ electrons is $L = 3$ and produces a disk shaped cloud of electrons with the orbital angular momentum J lying normal to the disk. This combined with the c/a

ratio of 1.59 for Tb (compressed along the c-axis compared to the hcp ideal of $c/a = 1.63$) creates a strong energy minimization for the electron cloud to have a normal perpendicular to the c-axis [9]. This effect is graphically illustrated in Figure 1.1. Since for Dy $c/a = 1.58$ and its $4f$ electron cloud has a radius within 2% of Tb [10], a similar effect and resulting anisotropy occurs for Dy as well.

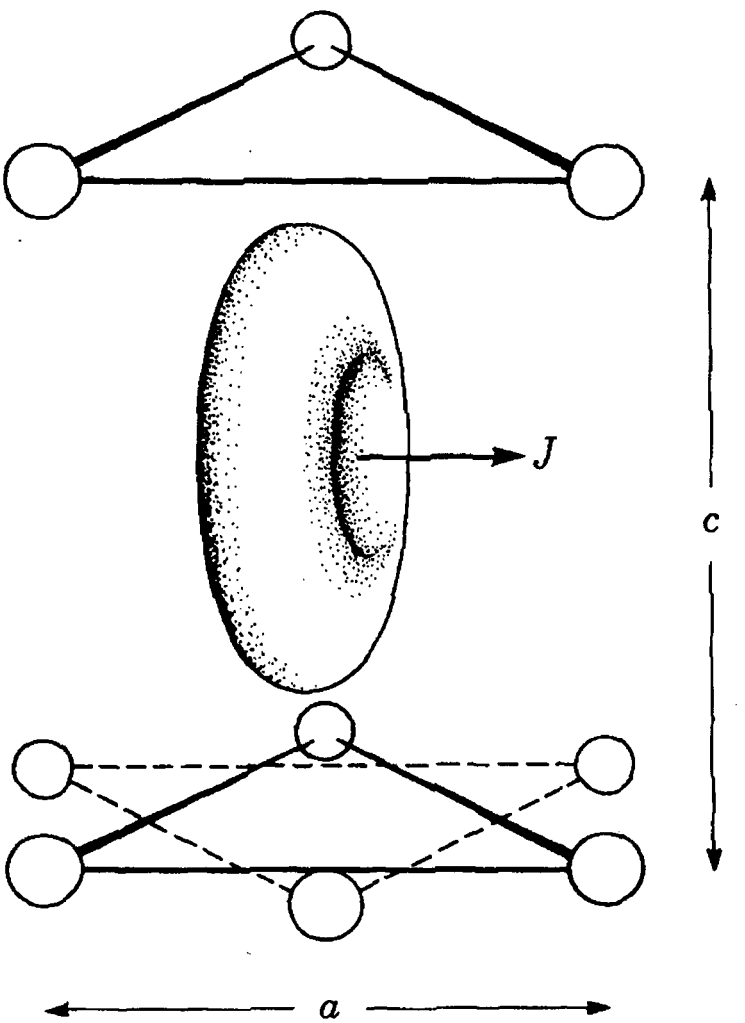

Figure 1.1: Electron cloud configuration of terbium in a hexagonal lattice. From Chikazumi [9].

1.4 Domain Influence on Magnetoelasticity

The analysis of magnetostriction and magnetocrystalline anisotropy to this point has assumed a simplified case of a single direction of magnetization. This case exists in reality only under extremely high external fields, as ferromagnetic materials generally form domains of magnetization below saturation. These domains consist of micromagnetic spins aligned parallel to each other, separated by Bloch walls which consist of layers of spins parallel to the interface of the domains and gradually rotating from one domain's orientation to the other's. (There exist domain walls at surfaces with other orientations, called Neel walls, but the effect of these are negligible for bulk materials.) To find the thickness of a Bloch wall, one minimizes the competing energy costs. The exchange energy in a domain wall is inversely proportional to the wall thickness while the anisotropy energy of the spins increases with wall thickness. Chikazumi [11] calculated the Bloch wall thickness for uniaxial materials (a close approximation to hard c-axis hexagonal materials such as TbDy) and found the thickness to be

$$\delta = \pi\sqrt{\frac{A}{K_2}} \tag{1.24}$$

with $A = nJS^2/a$, the magnetic stiffness constant, n as the number of atoms per unit cell, J as the exchange integral, S as the magnetic spins (3 for Tb, 5/2 for Dy, by Hund's rule), and a as the lattice constant. J can be computed using a mean-field theory:

$$J = \frac{3k_{\mathrm{B}}T_{\mathrm{c}}}{2zS\,(S+1)} \tag{1.25}$$

with z as the number of nearest neighbors. Typical values for δ are 150 lattice constants for iron.

Bloch walls may separate domains with oppositely oriented domains, called 180° walls, or domains with magnetizations normal to each other, called 90° walls (a term which also identifies domain walls separating magnetizations of other nonparallel orientations). Initially, the domain walls displace under magnetization such that domains pointing in the direction of increasing magnetization grow at the expense of other neighboring domains. Due to the hard c-axis hexagonal structure of TbDy, domains are assumed to always point in the basal plane. As a result, during magnetization 180° domain walls are not affected much since no energy reward with respect to magnetization energy is yielded. Meanwhile, 90° domain wall displacement provides the major source of magnetization and therefore net magnetostrictive strain. Once wall displacement is complete, the individual domains themselves must be rotated to provide further net magnetizations at higher applied fields. In many cases, material imperfections, polycrystal grain boundaries and other barriers to domain wall motion can force domain rotation during magnetization earlier than in the case of a perfect crystal, resulting in more difficult magnetizations and lower magnetoelastic strains. The importance of these phenomena in magnetoelastic damping will be discussed in Chapter 4.

1.5 Magnetoelastic Dissipation - Transformation of Elastic Energy into Magnetic Energy

The magnetoelastic behavior of ferromagnets is naturally coupled to applied stresses. When a ferromagnetic material is subject to an applied stress, its magnetization changes and energy is dissipated through various mechanisms, including domain wall width oscillation [12], domain wall motion and impedance and eddy currents [13]. Therefore, the induction of magnetization by applied stresses ultimately leads to dissipation of mechanical energy as heat.

Determining the magnetomechanical coupling of a material is necessary for a detailed description of its damping capabilities. The magnetoelastic coupling factor is the measure of a material's capacity to convert mechanical energy to or from magnetic energy [14]:

$$k = \frac{E_{\mathrm{me}}}{\sqrt{E_{\mathrm{e}} E_{\mathrm{m}}}} \tag{1.26}$$

with E_{me} being the magnetoelastic energy density and E_{e} and E_{m} being the elastic and magnetic energy densities. The magnetoelastic energy E_{me} can be derived using magnetoelastic tensors which relate terms of stress, strain, magnetic induction, magnetic field, magnetic permeability, and elastic compliance. These tensors take the form of

$$\delta\varepsilon = \mathbf{s}^{\mathbf{H}}\delta\tau + \mathbf{d}^{*}\delta\mathbf{H}, \quad \delta\mathbf{B} = \mathbf{d}\delta\tau + \boldsymbol{\mu}^{\tau}\delta\mathbf{H} \tag{1.27}$$

$$\delta\tau = \mathbf{c}^{\mathbf{H}}\delta\varepsilon - \mathbf{e}^{*}\delta\mathbf{H}, \quad \delta\mathbf{B} = \mathbf{e}\delta\varepsilon + \boldsymbol{\mu}^{\varepsilon}\delta\mathbf{H} \tag{1.28}$$

$$\delta\boldsymbol{\varepsilon} = \mathbf{s}^{\mathbf{B}}\delta\boldsymbol{\tau} + \mathbf{g}^{*}\delta\mathbf{B}, \quad \delta\mathbf{H} = -\mathbf{g}\delta\boldsymbol{\tau} + \boldsymbol{\nu}^{\tau}\delta\mathbf{B} \tag{1.29}$$

$$\delta\boldsymbol{\tau} = \mathbf{c}^{\mathbf{B}}\delta\boldsymbol{\varepsilon} - \mathbf{h}^{*}\delta\mathbf{B}, \quad \delta\mathbf{H} = -\mathbf{h}\delta\boldsymbol{\varepsilon} + \boldsymbol{\nu}^{\varepsilon}\delta\mathbf{B} \tag{1.30}$$

with $\mathbf{s}$ and $\mathbf{c}$ as the elastic compliance and stiffness tensors, $\boldsymbol{\varepsilon}$ and $\boldsymbol{\tau}$ as the stress and strain tensors, $\mathbf{d}$ and $\mathbf{g}$ as the piezomagnetic strain tensors satisfying $d_{ijk} = \partial B_k/\partial\tau_{ij}$ and $g_{ijk} = \partial H/\partial\tau_{ij}$, and $\mathbf{e}$ and $\mathbf{h}$ analogous piezomagnetic stress tensors. $\boldsymbol{\mu}$ is the magnetic permeability tensor and $\boldsymbol{\nu}$ is its inverse. In general, these tensors expand as four 9×9 elastomagnetic matrices which can be simplified for cases of high symmetry. By noting the

In general, expressions for E_{me} are complex in any non-isotropic ferromagnet, and this is especially the case for hexagonal symmetry [14]. Furthermore, such an expression neglects magnetoelastic effects arising from eddy currents, hysteresis, and other effects not considered in the terms of the magnetoelastic matrices and therefore are upper bounds on the efficiency of a material to transfer energy between elastic and magnetic states. Also, losses from dislocations and grain boundary interactions with magnetic domain formation and structure are not considered in this model.

As a result of these difficulties and shortcomings of the above direct approach toward magnetoelastic dissipation, more simplified approaches have been proposed. In one such model [15], an analogy is made between magnetoelastic dissipation and the magnetic hysteresis loop. The energy loss per cycle $\mathrm{d}U$ is represented by the magnetomechanical stress-strain hysteresis loop and is assumed to follow Rayleigh's law for small strains,

$$\Delta U = D\varepsilon^{3}, \ \varepsilon < \varepsilon_{\mathrm{c}} \tag{1.31}$$

with D as a constant and ε_{c} as the critical strain at which damping mechanisms are satu-

rated. Above ε_c, energy loss is a constant,

$$\Delta U = k\lambda E\varepsilon_c,\ \varepsilon \geq \varepsilon_c \tag{1.32}$$

with k a factor dependent on the hysteresis loop shape and is of the order of one in most cases. λ is the saturation magnetostriction in the direction of damping, and E is the elastic modulus. Therefore,

$$D = \frac{k\lambda E}{\varepsilon_c^2} \tag{1.33}$$

The value of this model is its ability to predict the critical strain and magnetostriction given the damping capacity $\Delta U/U$ of the material. Conversely, this model allows for comparison between measured saturation magnetostriction and critical strains with measured magnetomechanical hysteresis.

More sophisticated models of magnetoelastic damping attribute energy loss to irreversible domain jumps between axes of easy magnetization [15, 16]. This approach is useful for materials with multiple axes of easy magnetization such as Terfenol-D, a laves cubic phase TbDyFe alloy [16]. However, uniaxial symmetries with low magnetic anisotropy in the basal plane (as with TbDy) undergo continuous domain realignment in the basal plane and do not undergo symmetry-induced domain jumping. Application of these models to polycrystalline TbDy will be further discussed in Chapter 4.

1.6 TbDy - Magnetoelastic Properties

Most ferromagnetic materials have saturation magnetostriction strains of 10^{-4} to 10^{-6}. Iron, for example, has a magnetostriction strain in the (100) direction of 2.07×10^{-5} at room temperature; in the (111) direction, magnetostriction is actually negative, with contraction strains at saturation of -2.12×10^{-5}. The magnetostriction of rare earth elements and their alloys are often much greater than for most ferromagnets, however. Lowest-order basal plane magnetostriction constants $\lambda^{\gamma,2}$ for terbium and dysprosium approach 10^{-2} and can be compared with other materials of similar hexagonal symmetry in Table 1.2 [2, 3, 17, 18]:

Material	$\lambda^{\gamma,2}$ (ppm) @ 77 K
Co	55
Gd	125
Tb	7500
Dy	7000

Table 1.2: Basal plane magnetostriction constant $\lambda^{\gamma,2}$ for various hexagonal crystals

The magnetostrictive behavior of TbDy single crystals have been studied extensively and provide a simplified foundation of the more complex case of polycrystalline TbDy alloys. Single crystal rods of TbDy have been shown to have length magnetostriction of close to 1% at liquid helium temperatures [19]. At liquid nitrogen temperatures, $Tb_{0.5}Dy_{0.5}$ single crystals show peak magnetostrictive strains of 0.5% [20] and $Tb_{0.6}Dy_{0.4}$ samples are measured to have in excess of 0.6% saturation strains [21].

In the case of polycrystalline TbDy alloys, peak magnetostriction of hot-rolled $Tb_{0.6}Dy_{0.4}$ range up to 4000 ppm, approximately 70% of single crystal strains [21]. The

samples subjected to warmer annealing temperatures showed higher strains at all fields and stresses, usually an improvement of 25% for samples annealed at 1200 C vs. 700 C. This suggests an improvement of magnetostrictive performance due to increased grain growth at higher annealing temperatures. In addition, the elastic modulus of modulus at zero applied field of textured polycrystalline $Tb_{0.6}Dy_{0.4}$ samples was measured to be 15 GPa at applied stresses of 7 to 13 MPa.

In order to better understand the magnetoelastic behavior of polycrystalline TbDy, the effects of varying amounts deformation and annealing need to be explored. The study of texture in polycrystalline TbDy in relation to its thermal expansion anisotropy, magnetostriction and magnetomechanical damping properties provides a basis for this understanding.

Bibliography

[1] S. Chikazumi, *Physics of Ferromagnetism* (Clarendon Press, Oxford, 1997), p. 350.

[2] J. R. Cullen, Phys. Rev. B. **52**, 57 (1995).

[3] S. Ishio and M. Takahashi, J. Magn. Magn. Mater. **46**, 142 (1984).

[4] W. P. Mason, Phys. Rev. **96**, 302 (1954).

[5] J. J. Rhyne and S. Legvold, Phys. Rev. **138**, A507 (1965).

[6] M. L. Spano, A. E. Clark and M. Wun-Fogle, IEEE Trans. Magn. **25**,13794 (1989).

[7] J. J. Rhyne and A. E. Clark, J. Appl. Phys. **38**, 1379 (1967).

[8] C.-W. Chen, *Magnetism and Metallurgy of Soft Magnetic Materials* (Dover Publications, New York, 1986), p. 72.

[9] S. Chikazumi, p. 275-6.

[10] A. Freeman and R. Watson, Phys. Rev. **127**, 2058 (1962).

[11] S. Chikazumi, p. 411-6.

[12] Y. Liu and P. Grutter, J. Appl. Phys. **83**, 5922 (1998).

[13] K. B. Hathaway, A. E. Clark and J. P. Teter, Metal. and Mater. Trans. **26A**, 2797 (1995).

[14] E. du Tremolet de Lacheisserie, *Magnetostriction: Theory and Applications of Magnetoelasticity* (CRC Press, Boca Raton FL, 1993), p. 53-81.

[15] S. Laddha and D. C. Van Aken, Metal. Mater. Trans. **26A**, 957 (1995).

[16] G. W. Smith and J. R. Birchak, J. Appl. Phys. **40**, 5174 (1969).

[17] R. M. Bozorth and T. Wakiyama, J. Phys. Soc. Japan **18**, 97 (1963).

[18] A. E. Clark, B. F. DeSavage and R. M. Bozorth, Phys. Rev. **138** (1965), A216.

[19] M. L. Spano, A. E. Clark, J. P. Teter, and J. R. Cullen, Jour. de Phisique **49**, 347 (1989).

[20] M. L. Spano, A. E. Clark and M. Wun-Fogle, IEEE Trans. Magn. **26**, 1751 (1990).

[21] A. E. Clark, M. Wun-Fogle, J. B. Restoff and J. F. Lindberg, IEEE Trans Magn. **29**, 3511 (1993).

Chapter 2

Preparation and Thermal Expansion of Polycrystalline TbDy Samples

TbDy alloys have great potential as a material for use in cryogenic actuation and damping applications owing to large magnetoelastic effects. However, there exist practical barriers to their use owing to difficulties in preparation and undesirable mechanical properties, especially in the case of single crystals. This chapter addresses these issues and describes the preparation and analysis of polycrystal TbDy alloys used in our investigations. Our analysis here focuses on determination of texture through thermal expansion, optical metallography and x-ray diffraction for samples of various compositions and means of preparation.

2.1 Technical Advantages of Polycrystalline TbDy

The demand for magnetostrictive material development stems primarily from cryogenic actuation and damping applications. The development of the Next Generation Space Telescope (NGST) by NASA has been a primary source of interest in this technology. Giant magnetostrictive materials are particularly well suited for a proposed array of mirrors with reflected elements controlled by individual cryogenic actuators. In addition, the general need for vibration damping of spacecraft structures at cryogenic temperatures would be addresses by the magnetoelastic coupling of giant magnetostrictive materials such as TbDy alloys. Standard viscoelastic damping materials tend to stiffen and perform poorly when cold, and many common actuation materials such as piezoelectric crystals do not perform well at cryogenic temperatures. Inexpensive, high performance magnetostrictive materials therefore have the potential to perform a variety of functions in cryogenic applications.

In general, maximum linear magnetostrictive stroke for any ferromagnetic alloy is obtained by using a single crystal. Such is the case for TbDy, but growth of single crystals proves very difficult [1]. The binary phase diagram of TbDy alloys shows a cubic phase immediately below the melting temperature and above the low temperature hexagonal phase [2]. The high temperature cubic phase region makes it impossible to grow single crystals directly from the melt. As a result, the Materials Preparation Center at Ames, Iowa, prepares single crystals of TbDy by means of a strain-anneal preparation method. Unfortunately, this method produces sporadic results and is therefore suitable for production of samples in research quantities only. In addition, because impurities inhibit grain growth, high purity material is required for the single crystal growth process. *Commercial grade*

material has a typical purity of 99.7%, with the main impurities being Ta, O, and N, whereas the high purity material has a typical purity of 99.94%. High purity Tb (Dy) costs \$24/gm (\$9/gm) from Ames Laboratory Materials Preparation Center as compared to \$4/gm (\$1/gm) for commercial grade. This represents a considerable expense, as only a small portion of the starting material eventually becomes a single crystal suitable for use in devices, with the remainder contaminated in the process and therefore unsuitable for future attempts.

As a result of these difficulties in fabricating single crystals, the development of textured polycrystalline TbDy materials is necessary if this class of material is to be used for devices on a large scale. The texture describes the orientation of the individual crystallites in the material. Due to the elastic interactions of misaligned grains and the large anisotropy of the material, texture is critical to the magnetoelastic performance of polycrystalline TbDy. If crystallites are oriented at random in a solid the bulk magnetostriction is much smaller than for single crystals. Fortunately, deformation processes, such as rolling and drawing, can provide a strong crystallographic bias of the grain orientations in a solid. During deformation processing, damage is induced in the form of defects and dislocations and the material becomes work hardened. It is necessary to relieve some of the residual stress by heat treatment to obtain high performance magnetostrictive elements. While polycrystalline actuators generally exhibit reduced magnetostriction and may require somewhat larger applied magnetic fields for actuation, they also exhibit some clear advantages over single crystals. The primary practical advantage of using polycrystalline material is that commercial rolling and drawing processes are reliable and repeatable. Polycrystalline

materials can also be fabricated into a much greater range of shapes and sizes than can single crystals and can be tailored to produce a range of responses. In addition for single crystals it is necessary to include preload stresses in the design of devices in order to force the magnetization to return to its original state, whereas for polycrystalline TbDy alloys an applied stress is not as crucial [1,3]. The microstructural origin of this internal spring of polycrystals is likely related to elastic interactions between neighboring crystallites. It is possible that the need for a preload can be eliminated entirely by controlling the texture of the specimen. In contrast to the single crystals, the cost of preparation of the polycrystalline materials is as low as a few hundred dollars, with potential for further reductions when production techniques are optimized.

2.1.1 Preparation of Textured Polycrystalline TbDy Samples

Since Tb has an easy $\langle 10\bar{1}0 \rangle$ direction of magnetization while Dy has an easy $\langle 2\bar{1}\bar{1}0 \rangle$, an alloy ratio can be chosen to minimize the anisotropy in the basal plane for each temperature range of operation; for instance the estimated minima occur at $Tb_{0.76}Dy_{0.24}$ for 4 K, $Tb_{0.6}Dy_{0.4}$ for 77 K [4]. For production of polycrystals, the TbDy alloy is arc melted and dropped into a chilled cylindrical mold, creating an ingot about 4 cm long and 2.5 cm in diameter. The as-cast ingot shows strong radial texture, with grain growth outward from the central axis of the ingot. Such texture is clearly not suitable for magnetostriction, since the various grains will have magnetoelastic anisotropies in opposing directions. For purposes of magnetostriction of TbDy, the ideal case of a single crystal is best approximated by a polycrystalline alloy with grains oriented such that their hexagonal basal planes are close to parallel. Therefore, changing the texture of the samples through plastic deformation is

necessary. The texture of the material is critical due to the elastic interactions of misaligned grains and the large anisotropy of the material. At liquid helium temperatures a 10 Tesla field produces less than a 10% deflection from the basal plane [5]. In contrast to the single crystals, the cost of preparation of the polycrystalline materials is as low as a few hundred dollars, with potential for further reductions when production techniques are optimized.

In order to reduce the initial undesirable texture, our samples were first subjected to a deformation by plane rolling of 35% reduction in thickness, followed by a heat treatment at 950°C to induce recrystallization. The deformation randomizes the grain orientations, while the annealing at high temperature (approximately 500°C below the melting point) allows for further grain growth as well as strain relief. The net result is a sample suitable for more specific deformation, with a goal of a textured sample possessing a texture close to that of a single crystal. Sample 60c1 was prepared using flatter initial surfaces for rolling and was annealed at a higher temperature relative to other samples in order to produce more pronounced grain alignment. Samples for use in magnetostriction, damping and thermal expansion tests are then cut in rectangular shapes from the deformed ingots; a typical example is shown in Figure 2.1. Magnetostriction samples are typically 25 mm in length, 5 mm wide and 2 mm thick in order to fit into the measurement device. Damping measurement samples are not as long (1-1.6 cm) and thicker (4 mm thick) in order to prevent bending and to accommodate strain gauges. Thermal expansion measurement samples are approximately cubes 4 mm in height to for use in a thermal mechanical analyzer.

The specific samples and their various deformations and heat treatments are listed in Table 2.1. In general, the second deformation of our samples consisted of form rolling

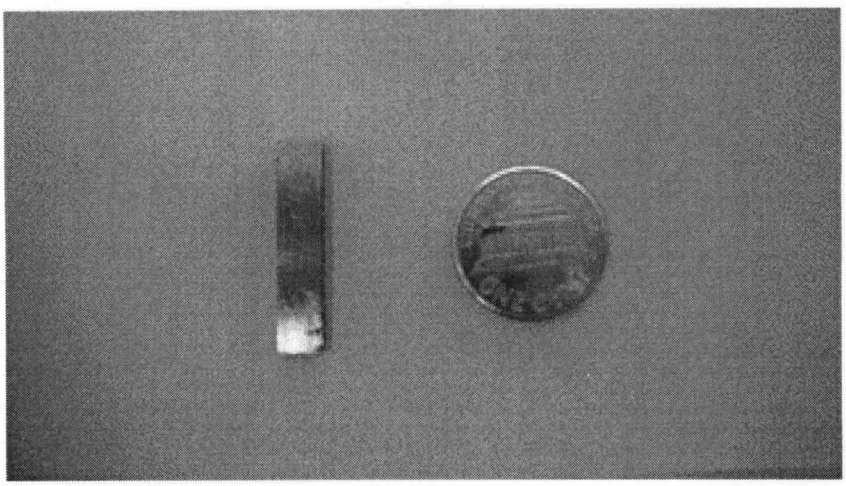

Figure 2.1: Sample of TbDy sized for magnetostriction tests.

or plane rolling by 0-55% and heat treatments of 350°C in order to relieve strain. The intent of these deformations was to take advantage of the natural tendency for hexagonal close packed crystals (of which TbDy crystals are a close approximation) to slip along their $[2\overline{1}\overline{1}0]$ direction, that is, along their basal planes [6]. Such slip lines can be seen in the upper section of Figure 2.2 as faint lines of contrast within a grain of TbDy. This dominant slip system of hexagonal TbDy will cause the normals of basal planes of the grains to point toward the direction of applied stress during plane rolling deformation. Since this corresponds to the hard axis of magnetization of TbDy, such texturing of our samples is clearly useful for improving magnetoelastic performance. The rolling and heating steps were varied for different samples in order to ascertain the benefits of larger deformations and longer annealing times. The deformation techniques used here are similar to commercial rolling and drawing processes. Therefore, practical applications of TbDy requiring flexible material properties and low costs will use alloys similar to those tested here.

Sample - Composition	First Rolling	First Anneal	Second Rolling	Second Anneal
76c1 - $Tb_{0.76}Dy_{0.24}$	35% plane	900°C, 1.5hr	55% plane	350°C, 1.5hr
76c2 - $Tb_{0.76}Dy_{0.24}$	35% plane	900°C, 1.5hr	25% plane ×4	350°C, 3hr ×4
76c3 - $Tb_{0.76}Dy_{0.24}$	35% plane	900°C, 1.5hr	55% plane ×2	350°C, 1.5hr ×2
76c4 - $Tb_{0.76}Dy_{0.24}$	35% plane	900°C, 2.5hr	20% plane	350-500°C, 1.5hr
76h1 - $Tb_{0.76}Dy_{0.24}$	35% plane	900°C, 1.5hr	55% plane	350°C, 1.5hr
60c1 - $Tb_{0.6}Dy_{0.4}$	35% plane	900°C, 1.5hr	20% plane	450°C, 1.5hr
60h1 - $Tb_{0.6}Dy_{0.4}$	35% plane	900°C, 1.5hr	25% plane ×4	350°C, 3hr ×4
60h2 - $Tb_{0.6}Dy_{0.4}$	35% plane	900°C, 1.5hr	55% plane	350°C, 24hr
60h3 - $Tb_{0.6}Dy_{0.4}$	35% plane	900°C, 1.5hr	10% plane	350°C, 1.5hr
60h4 - $Tb_{0.6}Dy_{0.4}$	35% plane	900°C, 1.5hr	55% plane×2	350°C, 1.5hr ×2
60h5 - $Tb_{0.6}Dy_{0.4}$	35% plane	900°C, 1.5hr	55% plane	350°C, 1.5hr

Table 2.1: Plane rolling and annealing of TbDy samples

2.1.2 Thermal Expansion measurements of TbDy

In order to better understand the texture of grains in our various samples of TbDy, we performed measurements of thermal expansion on both single crystal and polycrystal samples. The device used for these measurements was a Perkin Elmer thermal mechanical analyzer. The sample is in contact with a glass probe applying a preload of 50mN and immersed in a furnace. Measurements were taken in two temperature regimes: 300 K to 573 K, and 77 K to 300 K. For the first set of measurements, we used an inert atmosphere to prevent oxidation. The second set of tests employed a LN_2 dewar for cooling and allowed examination of thermal expansion as the samples cooled and warmed through the Curie and Neel points. Due to the strong magnetoelastic coupling of TbDy, interesting expansions and contractions occur at these magnetic transitions which were seen to be texture dependent.

The results for warm (300 - 573 K) thermal expansion measurements are shown in Table 2.2. Reduced anisotropy of thermal expansion for polycrystalline samples is evident compared to single crystal thermal expansion coefficients. This, along with unequal thermal

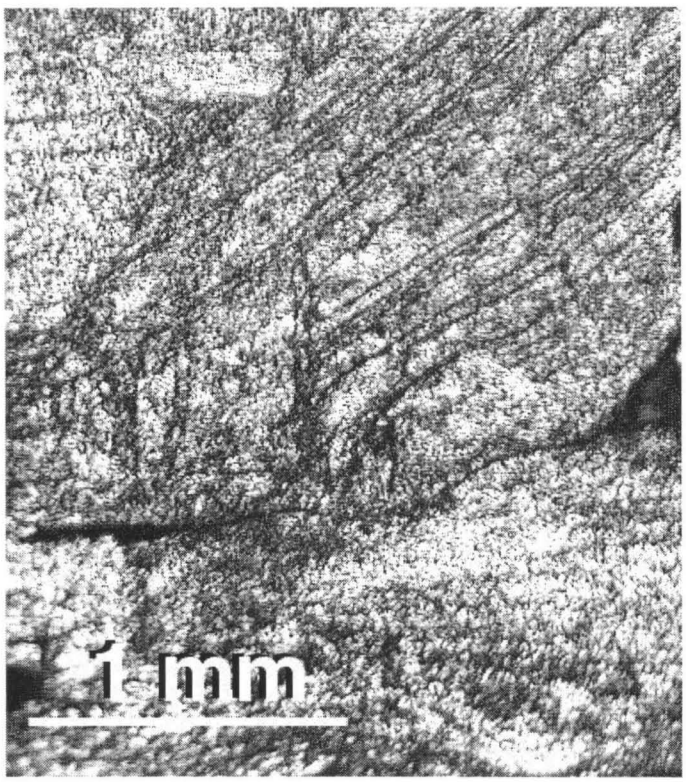

Figure 2.2: Optical micrograph showing slip lines within the grains of as deformed polycrystalline $Tb_{0.6}Dy_{0.4}$. The direction of applied stress of deformation is vertical in this image.

expansions along the rolling and transverse directions, indicates that texturing is far from complete. Nonetheless, the clear bias toward c-axis-like large thermal expansions in the axis of applied stress in deformation (the z-axis) confirms the existence of significant desirable texture

Further texture analysis was performed using thermal expansion from 300 K to 77 K. In this case, magnetomechanical effects could be seen as the samples underwent magnetic phase transitions. These effects make the data more difficult to quantify when compared to measurements above 300 K. However, some interesting effects of elastic coupling to

Sample - Composition	α, x-axis (10^{-6}/K)	α, y-axis (10^{-6}/K)	α, z-axis (10^{-6}/K)	$\alpha_{an} = \alpha_z/\alpha_x$
76c1 - $Tb_{0.76}Dy_{0.24}$	4.2	5.3	12.1	2.88
76c2 - $Tb_{0.76}Dy_{0.24}$	4.42	4.78	11.2	2.53
76c3 - $Tb_{0.76}Dy_{0.24}$	4.07	4.96	11.3	2.78
76h1 - $Tb_{0.76}Dy_{0.24}$	6.2	5.2	10.7	1.72
60h1 - $Tb_{0.6}Dy_{0.4}$	4.23	4.30	11.7	2.77
60h2 - $Tb_{0.6}Dy_{0.4}$	5.18	4.44	13.2	2.55
60h3 - $Tb_{0.6}Dy_{0.4}$	5.75	4.23	11.9	2.07
60h4 - $Tb_{0.6}Dy_{0.4}$	4.47	4.97	11.0	2.46
60h5 - $Tb_{0.6}Dy_{0.4}$	5.41	5.97	14.11	2.61
$Tb_{0.6}Dy_{0.4}$ single crystal	3.27	3.27	14.65	4.48

Table 2.2: Thermal expansion of polycrystalline TbDy samples, 30-300 C.

magnetization can be seen in this regime, including some effects related to texturing. Again, measurements were made for single element Tb and Dy single crystals, as well as single- and polycrystal alloys.

The thermal expansion properties around the Curie and Neel points of Tb and Dy can be seen in their respective single crystal thermal expansions in Figure 2.3. Of note are the thermal contractions with increasing temperature along the c-axis between the Curie and Neel points for both elements, as well as a residual contraction with increasing temperature even below the Curie point [7]. This is associated with the creation of antiferromagnetic, then ferromagnetic domains which align perpendicular to the hard axis of magnetization during cooling. Corresponding increases in expansion in the a- and b- directions at these temperatures were observed. The hysteresis associated with the heating-cooling cycles of these measurements is partially due to heating and cooling rates, but such hysteresis has been reported as an inherent property of these materials even for quasi-isothermal measurements [8].

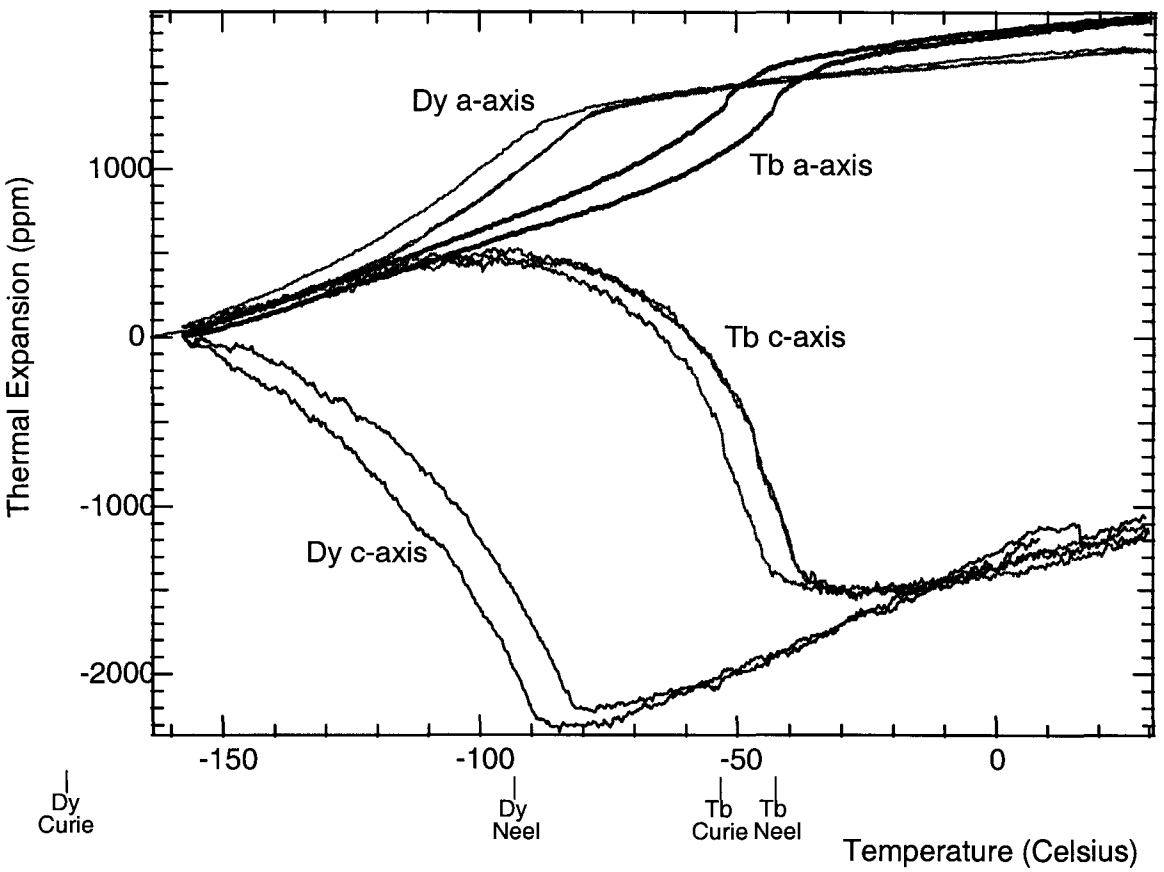

Figure 2.3: Thermal expansion properties about the Curie and Neel points of single crystal Tb and Dy. The Curie and Neel points of each element are noted below the x-axis of the graph.

The influence of deformation on the thermal expansion of TbDy has been shown to be especially apparent around the Curie and Neel points, clearly revealing instances of grain reorientations [9]. In the case of our rolled TbDy specimens, several effects of texture can be readily seen from cold thermal expansion measurements. Most striking was the difference between expansion in the rolling direction (x-axis) in Figure 2.4 and expansion in the direction transverse to rolling and applied stress (y-axis) in Figure 2.5. In particular, the x-axis shows behavior very similar to single crystal expansion in the basal plane, while

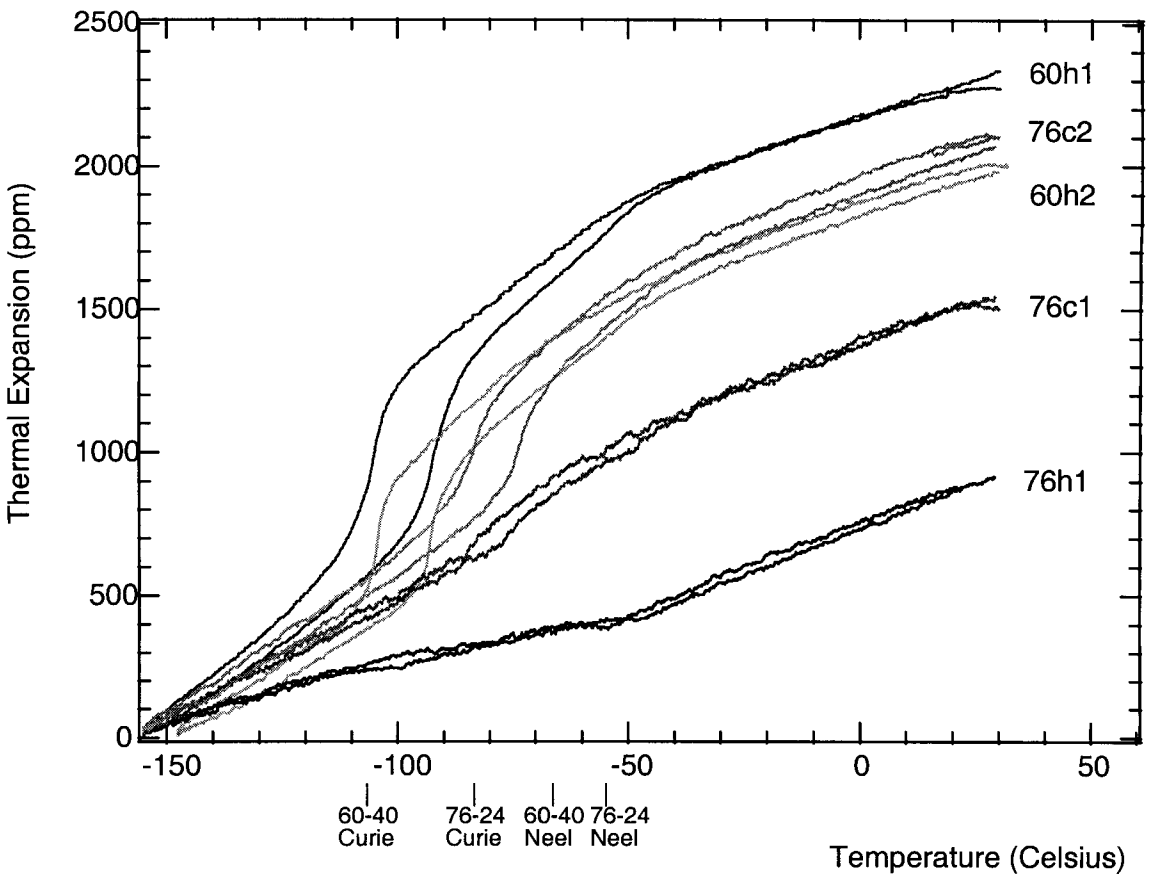

Figure 2.4: Cryogenic thermal expansion of TbDy polycrystalline samples along the axis of rolling (x-axis).

y-axis data show contraction near the Curie points of all but one sample (which showed a slowing of thermal expansion to near zero). This indicates a bias towards c-axis behavior in the rolling direction which is much more prominent than in the transverse direction. Such behavior is seen to some degree in all samples tested, though the least deformed and annealed samples 76h1 and 76c1 each had less pure a-axis-like thermal expansions in the x- and y-directions. As a result of this effect, the magnetic anisotropy of our samples of textured TbDy will not necessarily be minimized in the x-axis, which is the axis of

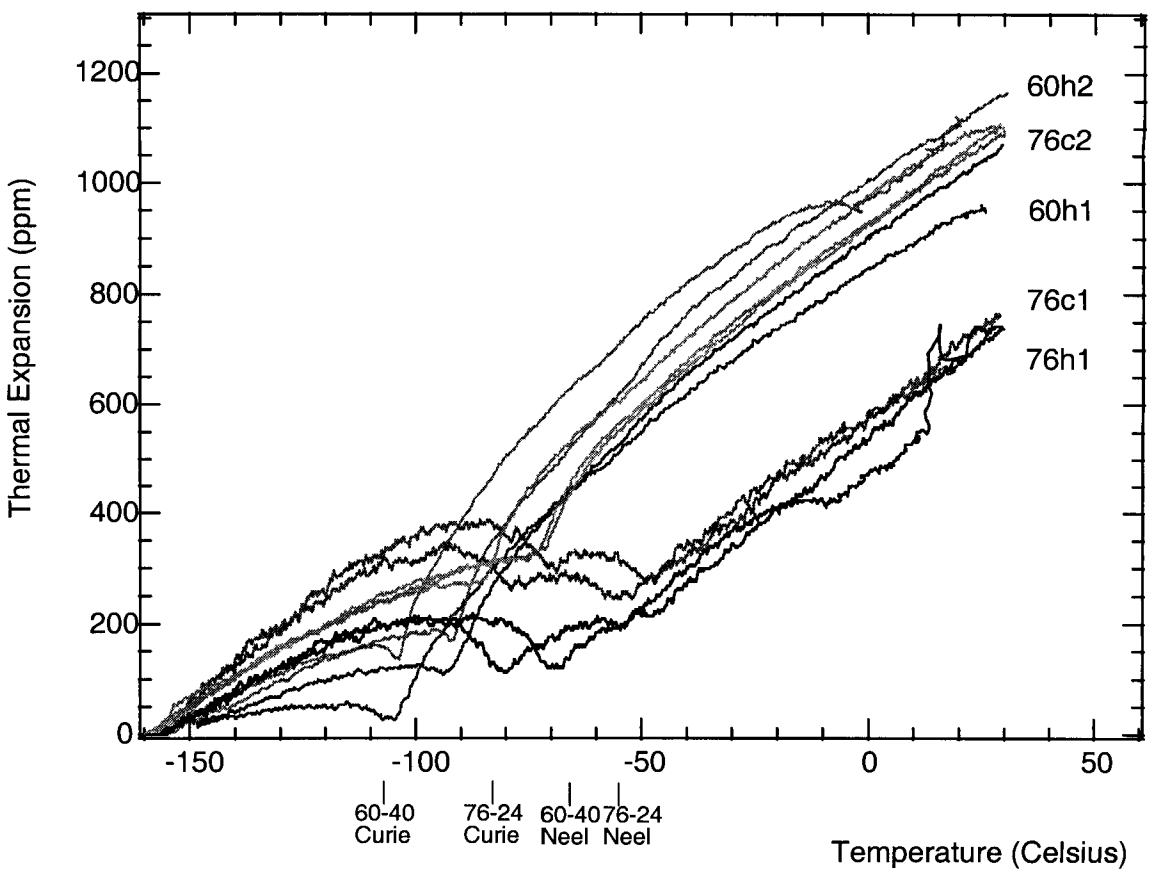

Figure 2.5: Cryogenic thermal expansion of TbDy polycrystalline samples along the axis transverse to the applied stress of deformation (y-axis).

magnetostrictive strain and of applied stress in the damping experiments of Chapters 3 and 4. Nonetheless, a more desirable grain orientation appears to exist in the x-axis compared to the texture in the y-axis. Measurements of the thermal expansion in the z-axes of our samples shown in Figure 2.6 reveals a large thermal contraction immediately below the Neel point, very similar to single crystal c-axis behavior. This result further confirms the strong tendency for the grains in our samples to orient their c-axes in the direction of applied stress of deformation.

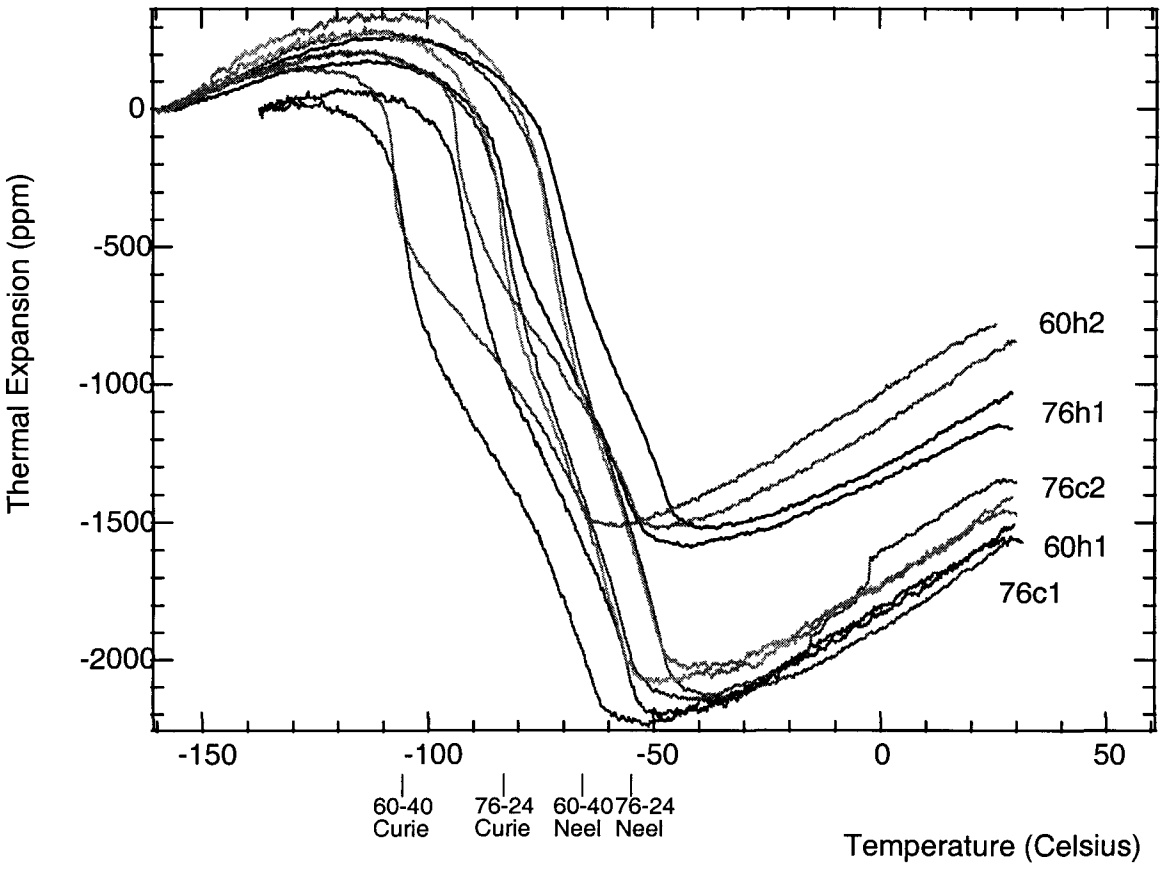

Figure 2.6: Cryogenic thermal expansion of TbDy polycrystalline samples along the axis transverse to the applied stress of deformation (z-axis).

Differences among the polycrystalline samples can be seen as well, most clearly the shifts in points of inflection for changing thermal expansion as a function of composition. Less clear are the differences in expansion as a function of deformation. In general, though, the samples with longer low-temperature annealing times seemed to have more pronounced anisotropy in expansion behavior. Comparisons of thermal expansion effects to magnetostrictive strain will be discussed in Chapter 3.

Bibliography

[1] A. E. Clark, M. Wun-Fogle, J. B. Restoff and J. F. Lindberg, IEEE Trans. Magn. **29**, 3511 (1993).

[2] K. A. Gschneidner and F. W. Calderwood, in *Handbook on the Physics and Chemistry of Rare Earths*, K. A. Gschneidner and L. Eyring, eds. (North-Holland, Amsterdam, 1986), p. 1.

[3] M. L. Spano, A. E. Clark and M. Wun-Fogle, IEEE Trans. Magn. **26**, 1751 (1990).

[4] M. L. Spano, A. E. Clark and M. Wun-Fogle, IEEE Trans. Magn. **25**, 13794 (1989).

[5] J. J. Rhyne and A. E. Clark, J. Appl. Phys. **38**, 1379 (1967).

[6] C. Barrett, *Structure of Metals* (McGraw-Hill, New York, 1952) p. 336-7.

[7] B. J. Beaudry and K. A. Gschneidner and F. W. Calderwood, in *Handbook on the Physics and Chemistry of Rare Earths*, K. A. Gschneidner and L. Eyring, eds. (North-Holland, Amsterdam, 1986), p. 173.

[8] E. B. Amitin, W. G. Bessergenev and Y. A. Kovalevskaya, J. Chem. Thermo. **16**, 959 (1984).

[9] S. M. Barmin, S. V. Kortov and P. V. Gel'd, Sov. Phys. Solid State **33**, 1560 (1991).

Chapter 3

Magnetostriction of Textured TbDy Alloys

In this chapter we present the measurement and analysis of magnetostriction measurements of bulk polycrystalline TbDy alloys. First, the measurement instrumentation will be described, then magnetostriction data of TbDy alloy samples of various texture and composition, including single crystal control samples, will be shown. Finally, analysis of the saturation strain, applied stress dependence, hysteresis and texture dependence of magnetostriction are discussed.

3.1 Magnetostriction Measurements of TbDy

Many of the primary technological applications of TbDy alloys require the use of liquid nitrogen as a cooling agent, as this is the most convenient and inexpensive agent for cooling of devices below 100 K. Therefore, our primary set of measurements were performed

at 77K in a LN_2 bath. Each sample was cut rectangularly with a long axis parallel to the direction of rolling. Since the texture of our samples is such that the *c*-axis of the grains points in the direction of deformation as shown by our thermal expansion results, the long axis of each resulting sample is an approximate easy axis of magnetization. The sample fits into a slot drilled into one arm of the fiberglass calipers shown in Figures 3.1-3.2. The ends of the sample were in contact with aluminum plates attached to each arm of the measurement device. As the calipers closed, the sample was thus held in place with a normal force on each end of the sample. A high-tension string attached to one arm of the calipers pulled the arms together when the string was pulled away from the calipers, thus applying a force to the sample. By attaching the string to a pulley and hanging a known weight off of the free end of the string, a load could be applied to the sample varying from 0-45 MPa. This applied load interacts with the magnetoelastic coupling of the sample to induce domain alignment perpendicular to the long axis of the sample [1].

The ends of the calipers were placed in a LN_2 dewar such that the sample was totally immersed. Opposite either end of the sample were poles of an electromagnet capable of varying fields up to 4.5 kOe. The applied field was along the length of the sample so as to magnetization, and hence expansion, in the direction of the length of the sample. A capacitance gauge capable of resolution to 0.03 mm was mounted within the calipers adjacent to the sample and measured linear displacement between the calipers caused by the sample's magnetostrictive strain.. The electromanget's induced field was controlled by a PC computer connected to a National Instruments data acquisition card. A purpose-developed LabView software module coordinated simultaneous signal output and capacitance gauge

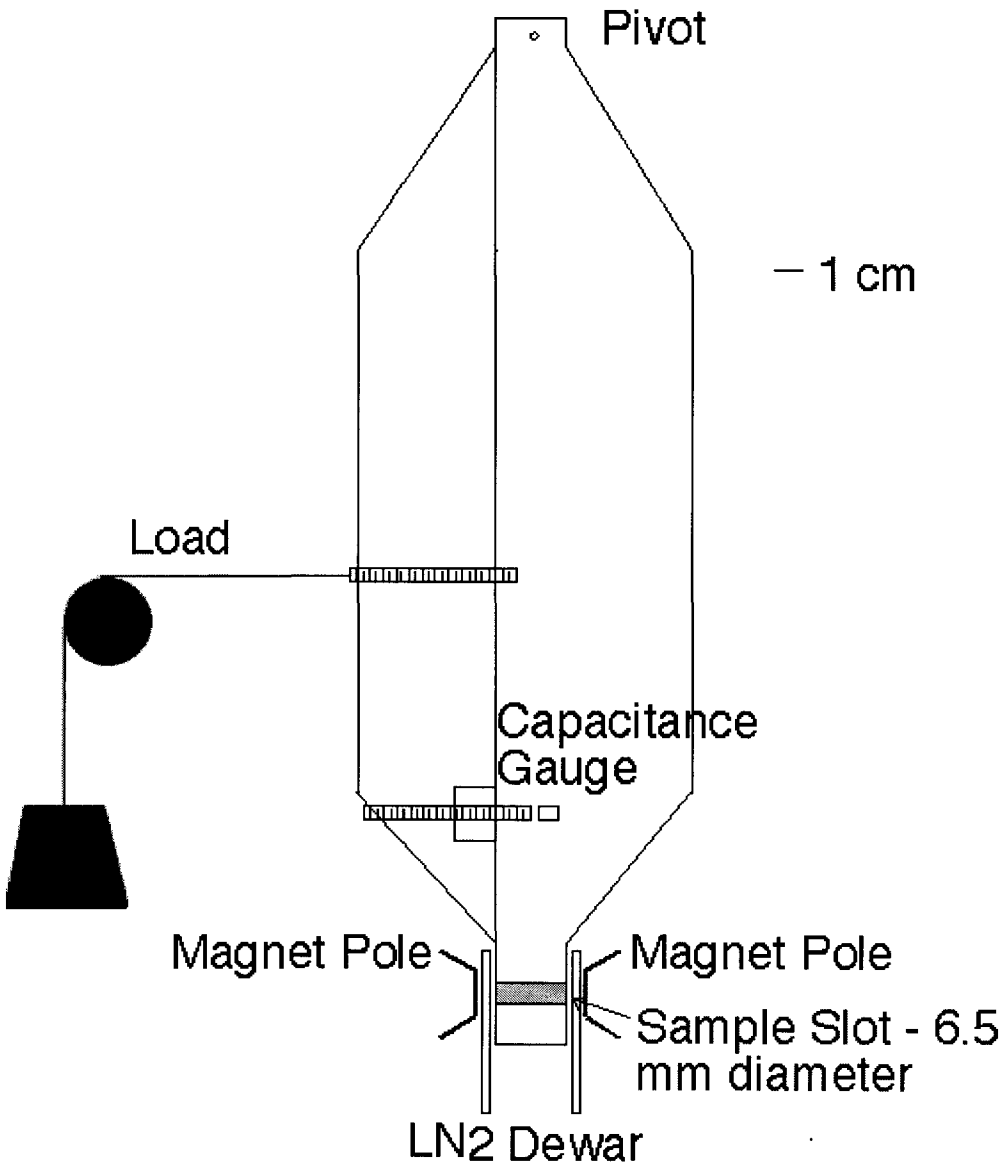

Figure 3.1: Device for measurements of TbDy magnetostriction at 77 K.

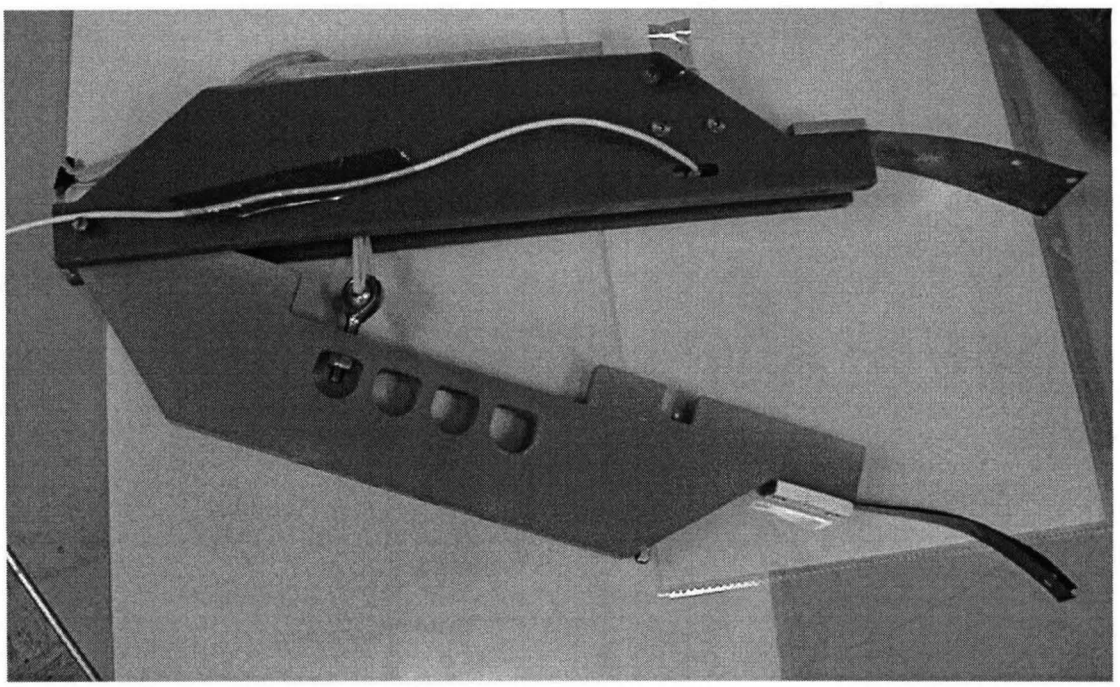

Figure 3.2: Photo of the magnetostriction measurement device. Here, the calipers are swung open for sample loading. The white cable taped to the top caliper leads to the capacitance gauge probe.

input, with the data acquisition card performing analog-to-digital conversions as needed. Direct measurement of the applied field during magnetostriction measurements proved difficult due to the tight confines of our electromagnet poles, LN_2 dewar and measurement apparatus. Therefore, indirect measurements were made by calibrating input current versus field. The final result is a hysteresis curve of magnetostrictive stroke versus applied field.

A typical set of strain-field hysteresis loops for sample 60h5 of $Tb_{0.6}Dy_{0.4}$ at varying applied loads is shown in Figure 3.3. This sample has composition optimized for minimum basal-plane magnetocrystalline anisotropy at 77 K [1]. Several properties of polycrystal TbDy are notable in this figure. First, the saturation field for magnetostriction occurs above 4.5 kOe (our device limit) for our polycrystalline samples. The highest magnetostric-

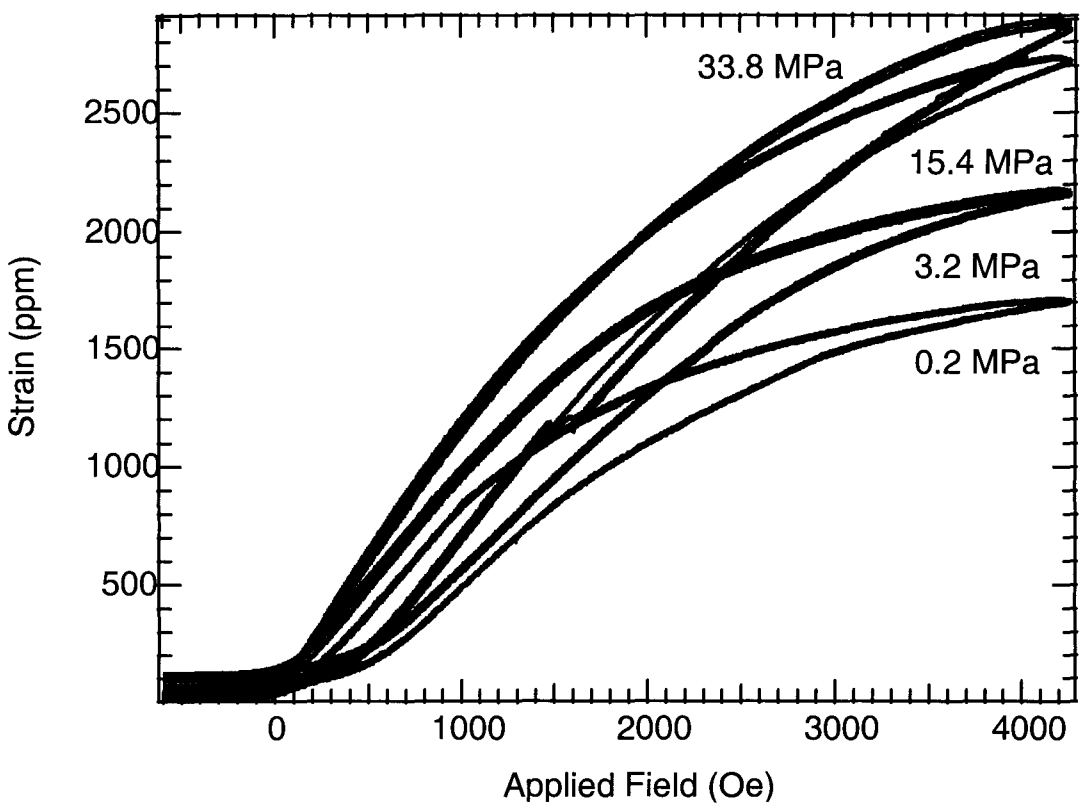

Figure 3.3: Magnetostrictive strain versus applied field for polycrystalline $Tb_{0.6}Dy_{0.4}$ at various applied loads.

tion attained for this sample was approximately 2900 ppm at 33.8 MPa of applied load. Approximately 90% of this maximum strain was obtained with a preload of 15.4 MPa and 75% of the maximum strain was obtained with a minimal 3.2 MPa preload. The ability to achieve significant percentages of maximum magnetostrictive stroke with minimal preload is peculiar to polycrystalline TbDy, as single crystals require a preload to re-rotate the magnetization into the basal plane [2]. Evidently there exists an internal spring mechanism induced by intergrain elastic interactions. More thorough texture analysis and measurements of internal strains of TbDy polycrystals are needed in order to better understand

this phenomena. Also notable is the near-complete independence of the width of the magnetostriction hysteresis curve with respect to changing applied loads, an effect observed for each of our samples. This is consistent with previous experimental results of TbDy single crystals [2] and hot-rolled grain oriented sheets [3], as well as simulations of complex TbDyFe magnetostrictive structures [4].

In general, the shape of the magnetostriction hysteresis curves of single crystal TbDy alloys is dictated by the basal plane anisotropy K_6^6 [2]. While much smaller than the c-axis anisotropy, K_6^6 is nonetheless large even when minimized for a particular temperature by composition, as noted in Chapter 2. In particular, minima of magnetocrystalline anisotropy are located 60 degrees apart in the basal plane of TbDy crystals. Therefore, single crystal TbDy magnetostriction shows a kink where this energy barrier is overcome by the applied field. This effect is most apparent for compositions of TbDy not optimized for minimum anisotropy [2], but is almost completely absent when K_6^6 is minimized. Since slip planes of hexagonal materials show no preference for orientation of a- or b- axes of grains [5], we expect this effect to be attenuated for textured polycrystalline TbDy samples. Indeed, we see no analogous abrupt change in the slope of magnetostriction versus field curves, confirming the randomization of a- and b- axes of our grains.

While each of our polycrystalline TbDy samples exhibited similar magnetostrictive behavior, some differences were noted as functions of sample preparation. Most obvious and expected was generally higher magnetostrictive strains for the $Tb_{0.6}Dy_{0.4}$ samples at 77 K, since such samples had a Tb:Dy composition ratio optimized for this temperature. Nonetheless, other factors heavily influenced magnetostrictive performance. First, our sam-

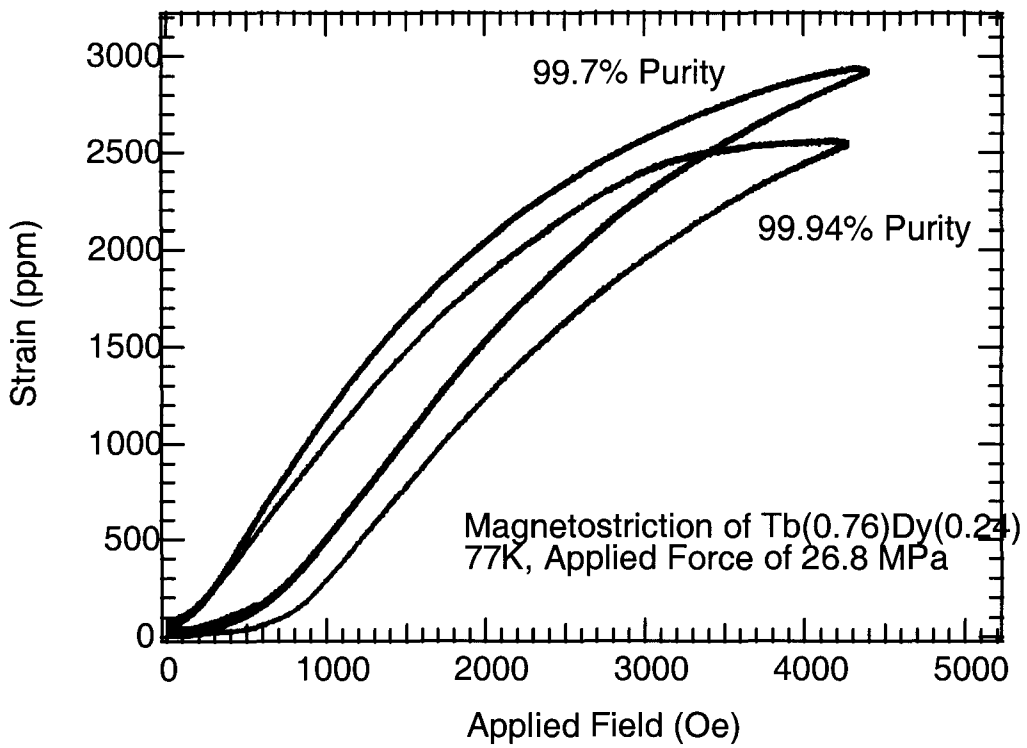

Figure 3.4: Magnetostriction of commercial purity versus high purity polycrystalline $Tb_{0.76}Dy_{0.24}$.

ples were of two purities: commercial (99.4%) and high (99.97%). We noticed a consistent pattern of increased strains from commercial purity specimen 76c1 versus otherwise identically prepared high purity 76h1 specimen. A typical case is presented in Figure 3.4. High strains were also measured for the commercial purity sample 60c1 relative to other $Tb_{0.6}Dy_{0.4}$ samples. Second, the effects of preload on magnetostrictive performance varied largely between samples. The only trend clear from all samples tested was a large increase in magnetostrictive stroke (usually 30-40%) between small (<5 MPa) preloads to larger (>10 MPa) preloads, with a smaller effect for larger preloads up to ~36 MPa. A graphical

summary of maximum magnetostrictive stroke versus preload can be seen in Figures 3.5-3.6.

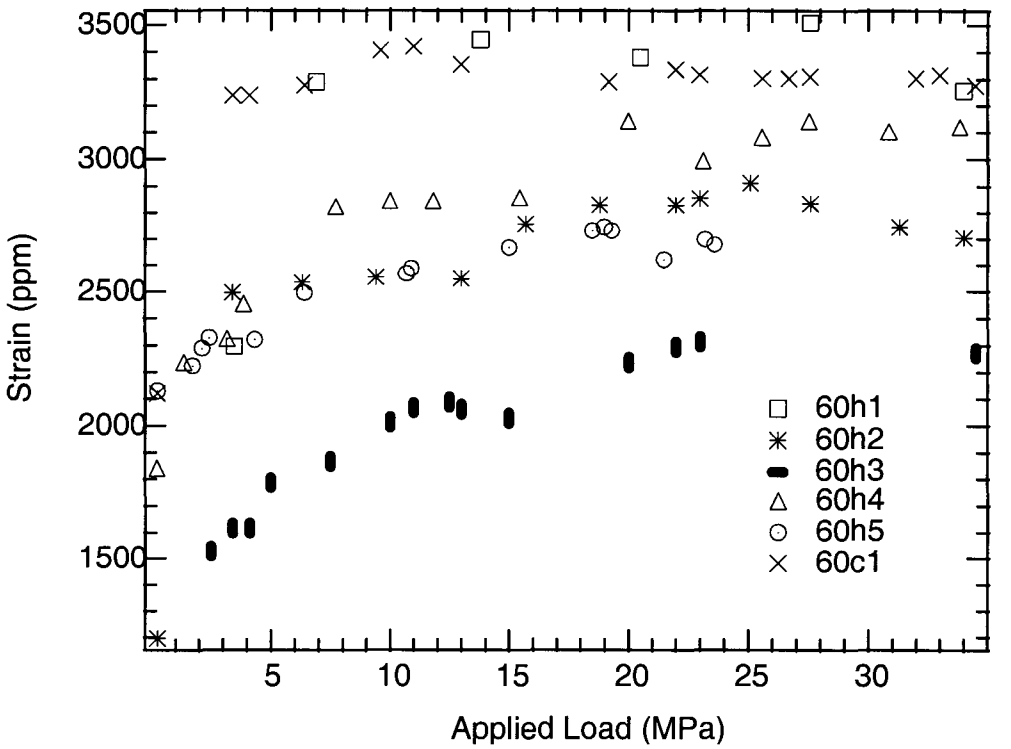

Figure 3.5: Summary of magnetostriction measurements of polycrystalline $Tb_{0.6}Dy_{0.4}$.

The highest measured magnetostrictions of $Tb_{0.6}Dy_{0.4}$ samples occur for 60c1 and 60h1, each of which was prepared so as to produce more grain alignment compared to the other $Tb_{0.6}Dy_{0.4}$ samples. The smallest strains were measured for the least deformed sample, 60h3. These trends were not as clear for $Tb_{0.76}Dy_{0.24}$ samples. The strain measurements of $Tb_{0.6}Dy_{0.4}$ samples compare reasonably well to previous work with hot-rolled sheets, except insofar as high purity hot-rolled sheets outperformed commercial grade specimen. This discrepancy can be accounted for by the preferential growth of highly oriented grains during 25-fold hot-rolling. In contrast, our cold-rolled samples experienced growth of more

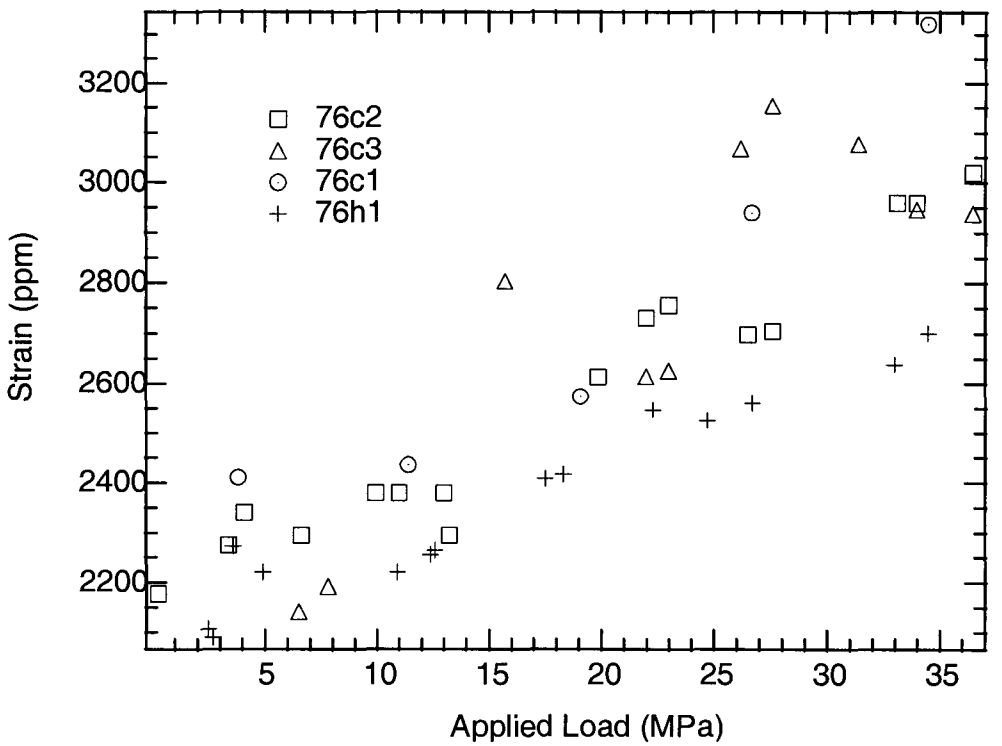

Figure 3.6: Summary of magnetostriction measurements of polycrystalline $Tb_{0.76}Dy_{0.24}$.

randomized grains during the initial anneal before the primary texturing deformation.

3.2 Magnetostrictive Performance over Multiple Cycles

A key property of any candidate material for applications in actuator devices is resistance to deterioration over multiple duty cycles. In order to ascertain the magnetoelastic fatigue of polycrystalline TbDy, we measured magnetostrictive strain over multiple cycles of expansion. The results of 155 cycles of expansion of a sample of $Tb_{0.6}Dy_{0.4}$ can be seen in Figure 3.7. In this case, the sample was subjected to fields of $0 - 4.2$ kOe cycling at 0.1 Hz for over 25 minutes, with an applied load of 20.5 MPa so as to produce a high ($\sim$ 3000

ppm) strain. The maximum change in strain during the experiment is approximately 50 ppm, within the range of error of the experimental apparatus from such sources as thermal drift and condensation. Other samples showed similar behavior, with fatigues within measurement errors. Clearly, polycrystalline TbDy alloys are resilient to fatigue over multiple cycles.

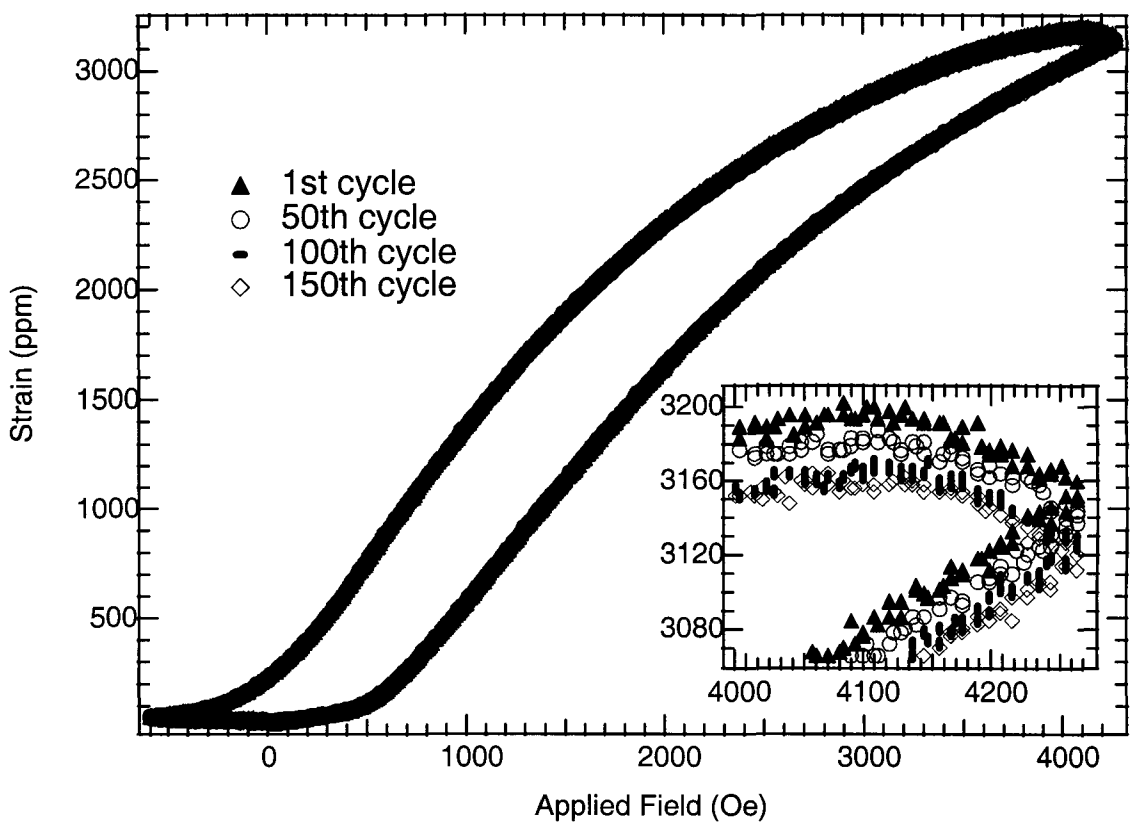

Figure 3.7: Magnetostriction of polycrystalline $Tb_{0.6}Dy_{0.4}$ over 150 cycles.

3.3 Magnetostriction vs. Thermal Expansion Anisotropy

As discussed in Chapter 2, thermal expansion measurements of TbDy polycrystals provide information on grain alignment. Specifically, the degree to which the c-axes of grains align themselves in a particular direction in a sample can be determined by comparing thermal expansion to known single crystal values. Of particular interest in our investigation is the ratio of thermal expansions in the z- and x- directions as they provide a measure of grain alignment along the direction of magnetostriction, the x-axis. This ratio is termed the thermal expansion anisotropy, $\alpha_{\text{an}} = \alpha_z/\alpha_x$.

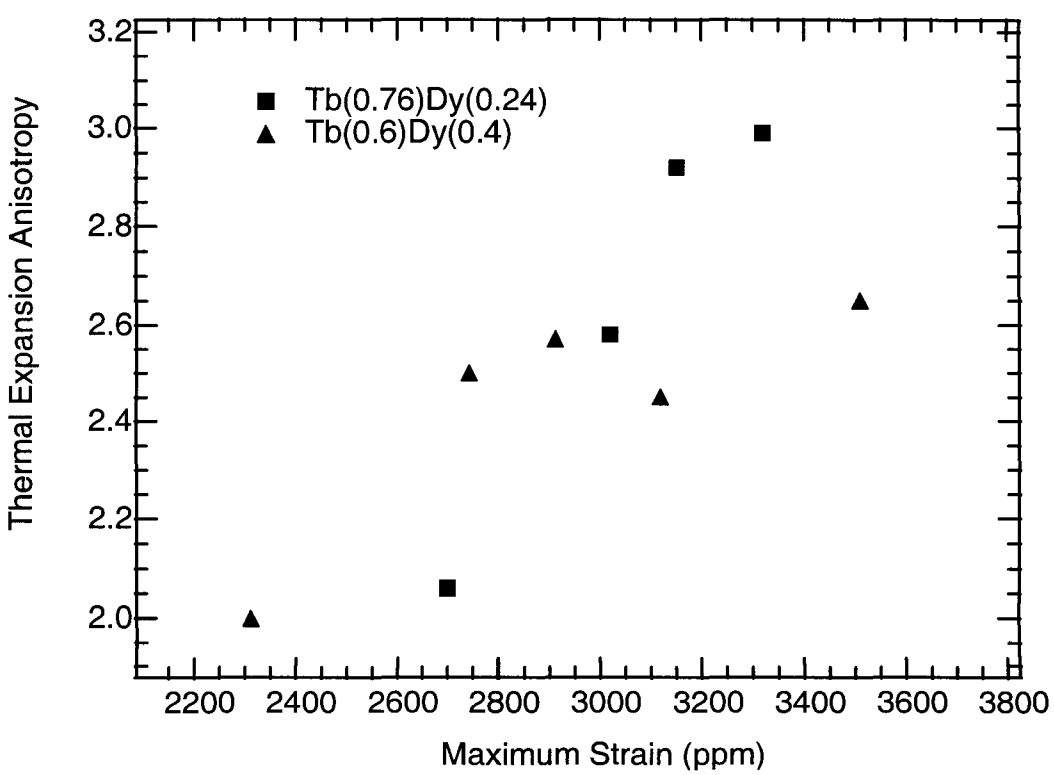

Figure 3.8: Magnetostriction versus thermal expansion anisotropy.

Figure 3.8 shows the thermal expansion anisotropy α_{an} versus maximum magnetostrictive stroke for several samples of polycrystalline TbDy. Differences in α_{an} between single crystals of $Tb_{0.6}Dy_{0.4}$ and $Tb_{0.76}Dy_{0.24}$ have been accounted for when calculating α_{an} for polycrystalline samples. The samples with the more highly anisotropic thermal expansions generally have the higher peak magnetostrictions. In addition, the highest values of α_{an} occur for commercial purity samples 76c1, while identically prepared 76h1 has a low value of α_{an} and correspondingly low magnetostriction. Meanwhile, the least deformed sample, 60h3, has a very low α_{an} of ~ 2.0. For comparison, a single crystal of $Tb_{0.6}Dy_{0.4}$ has thermal expansion anisotropy $\alpha_{an} = \alpha_c/\alpha_a = 4.48$ and maximum magnetostrictive strain of approximately 6200 ppm [3].

A closer look at values of α_{an} and magnetostriction performance for samples 76c2 and 60h1 reveals an interesting result. For 76c2, $\alpha_{an} = 2.38$ and for 60h1, $\alpha_{an} = 2.65$. Each of these samples were deformed and annealed four times during texturing in an effort to produce better grain alignment normal to the axis of deformation. While each sample produces consistently high magnetostriction relative to samples of similar composition and different preparation, each has values of α_{an} which are not higher than other samples. Evidently, this multi-step deformation-annealing process does not aid grain reorientation yet improves magnetostrictive performance more than their values of α_{an} would suggest. This result implies the existence of important correlations between magnetoelastic performance and second-order magnetomechanical interactions with grains and grain boundaries in polycrystalline TbDy meriting further study.

3.4 Influence of grain orientation on magnetic energy

Higher energies of magnetization are required in directions of large magnetocrystalline anisotropy. Therefore, the energy needed to magnetize TbDy alloys is dependent on texture and its effects on magnetocrystalline anisotropy. In an effort to better understand this relationship, we developed a model relating magnetization energy to texture for polycrystalline TbDy alloys.

For hexagonal materials with a dominant first order K_2 coefficient of hard c-axis magnetic anisotropy as with TbDy, we can approximate the energy of magnetization as [6]

$$E \cong K_2 \sin^2 \theta \tag{3.1}$$

with θ as the angle of magnetization out of the basal plane, and $K_2 = 5.3 \times 10^8$ erg/cm^3 for $Tb_{0.6}Dy_{0.4}$. There exist contributions to this energy from higher order c-axis terms and from magnetic anisotropy in the basal plane as discussed in Chapter 1, but such factors are negligible for TbDy. Since we apply a field in the x-direction during magnetostriction measurements, grains with their c-axes oriented away from the sample's z-axis by an angle θ have internal energies in accordance with Equation 3.1. The estimated internal magnetic energy of a sample at magnetic saturation can therefore be calculated by knowing the angular grain distribution.

We can use the thermal expansion anisotropy to estimate the angular distribution of grains in TbDy polycrystals. By using the method of Roe [7] and Dunn and Ledbetter [8], we calculated orientation distribution coefficients W_{200} and W_{220} in the approximation:

$$w(\theta) \cong \frac{W_{200}}{2}\left(3\cos^2\theta - 1\right) + 3W_{220}\sin^2\theta \tag{3.2}$$

The probability density $w(\theta)$ of grains at an angle θ from the z-axis is strictly calculated with more terms of W_{lmn}, but the two terms used here are the only ones which can be derived from thermal expansion. W_{200} and W_{220} were calculated from the following:

$$W_{200} = \left[\frac{3}{8\sqrt{2/5}\pi^2\left(\alpha_c^{sc} - \alpha_a^{sc}\right)}\right]\left[\alpha_z^r - \frac{2\left(\alpha_c^{sc} + \alpha_a^{sc}\right)}{3}\right] \tag{3.3}$$

$$W_{220} = \left[\frac{\sqrt{15}}{8\pi^2\left(\alpha_c^{sc} - \alpha_a^{sc}\right)}\right]\left[\alpha_x^r - \frac{2\left(\alpha_c^{sc} + \alpha_a^{sc}\right)}{3} + \frac{4\sqrt{2/5}\pi^2\left(\alpha_c^{sc} - \alpha_a^{sc}\right)}{3}W_{200}\right] \tag{3.4}$$

We normalized $w(\theta)$ and integrated the grain distribution multiplied by the energy of magnetization in Equation 3.1 to obtain an estimate of the magnetic energy due to magnetocrystalline anisotropy

$$E_K = \int_0^{\pi/2} w(\theta) \times K_2 \sin^2\theta \, \mathrm{d}\theta \tag{3.5}$$

The results of our analysis are presented in Figure 3.9. The trend seen in our results generally shows lower internal energies of magnetization corresponding to higher magnetostriction, in agreement with our measured relationship between magnetostriction and thermal expansion anisotropy. (An inconsistent result exists for sample 60c5 due to an anomalous z-axis thermal expansion result.)

The grain orientation measurement here is incomplete, as only two orientation distribution coefficients are used. Also, this model ignores grain sizes and their effect on the grain distribution, as well as magnetic domain interactions with grain boundaries. More

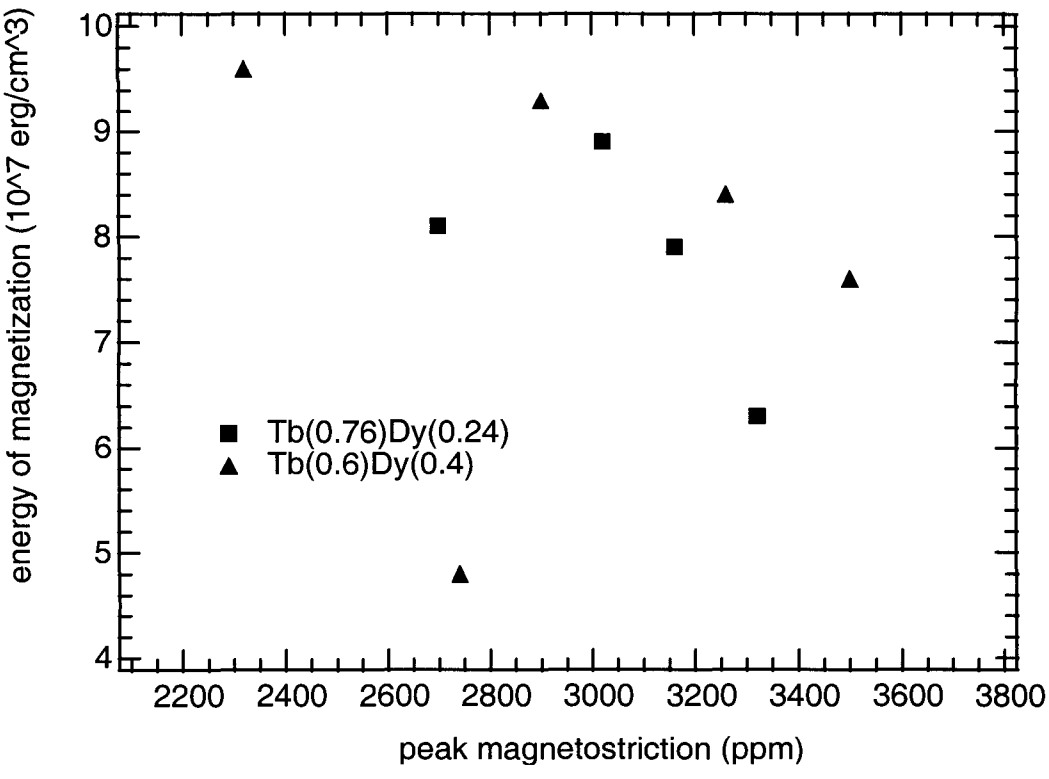

Figure 3.9: Energy of magnetization versus peak magnetostriction for polycrystalline TbDy samples.

detailed measurements of the texture of TbDy alloys would improve the usefulness of this model and likely would yield insight into microstructural influences on magnetostriction.

Bibliography

[1] J. J. Rhyne and A. E. Clark, J. Appl. Phys. **38**, 1379 (1967).

[2] M. L. Spano, A. E. Clark and M. Wun-Fogle, IEEE Trans. Magn. **26**, 1751 (1990).

[3] A. E. Clark, M. Wun-Fogle, J. B. Restoff and J. F. Lindberg, IEEE Trans Magn. **29**, 3511 (1993).

[4] R. James, D. Kinderlehrer and L. Ma, in *Mathematics of Microstructure Evolution*, edited by L. Q. Chen, B. Fultz, J. W. Cahn, J. R. Manning, J. E. Morral and J. A. Simmons (The Minerals, Metals and Materials Society, Warrendale PA, 1996), p. 56.

[5] C. Barrett, *Structure of Metals* (McGraw-Hill, New York, 1952) p. 336-7.

[6] S. Chikazumi, *Physics of Ferromagnetism* (Clarendon Press, Oxford, 1997), p. 249.

[7] R. J. Roe, J. Appl. Phys. **36**, 2024 (1965).

[8] M. L. Dunn and H. Ledbetter, J. Appl. Phys. **78**, 1583 (1995).

Chapter 4

Magnetomechanical damping by polycrystalline TbDy

Magnetostriction under an applied field is one side of the symmetrical relationship between magnetization and stress in ferromagnetic materials. As a ferromagnetic alloy is strained, mechanical energy is converted into magnetic energy through domain realignment and domain wall motion. The net result of this effect is magnetomechanical damping. In this chapter, we present results of investigations into the magnetomechanical damping properties of polycrystalline TbDy.

4.1 Introduction

The large magnetomechanical coupling of TbDy alloys detailed in Chapter 1 allows for realignment of domains under applied mechanical stresses. Because these effects occur at temperatures below the Curie point, TbDy alloys lend themselves to cryogenic damping

applications. Previous studies of materials with large magnetostrictions show considerable mechanical hysteresis due to magnetoelastic effects, often dissipating upwards of 25% of the mechanical energy at zero applied field in the case of polycrystalline Terfenol-D [1]. In addition, samples with more well-defined texture dissipated more energy per cycle, with texture playing a more prominent role at lower applied strains.

Previous work with damping properties of TbDy alloys has been limited. Notably, the elastic modulus of modulus at zero applied field of textured polycrystalline $Tb_{0.6}Dy_{0.4}$ samples was measured to be 15 GPa at 77K and applied stresses of 7 to 13 MPa [2]. This is much lower than the elastic modulus of Tb and Dy above the Curie point, typically between 20 and 70 GPa for single crystals depending on crystallographic direction [3, 4]. Clearly, ferromagnetism has a large influence on the elastic properties of TbDy, an issue that will be addressed in this chapter.

4.2 Measurement of Stress-Strain Relations of Polycrystalline TbDy

In order to determine the magnetomechanical behavior of TbDy polycrystalline alloys, we measured the stress-strain curves of samples at multiple ranges of applied stresses. We utilized an Instron load frame which provides a constant vertical motion of a flat surface over the samples. This surface is attached to a load cell which measures the applied stress on the sample. Strain gages were affixed to the TbDy samples to measure strains along the sample's x-direction as in Figure 4.1.

We chose the samples 76c1 and 76h1 for our tests, due to their markedly different

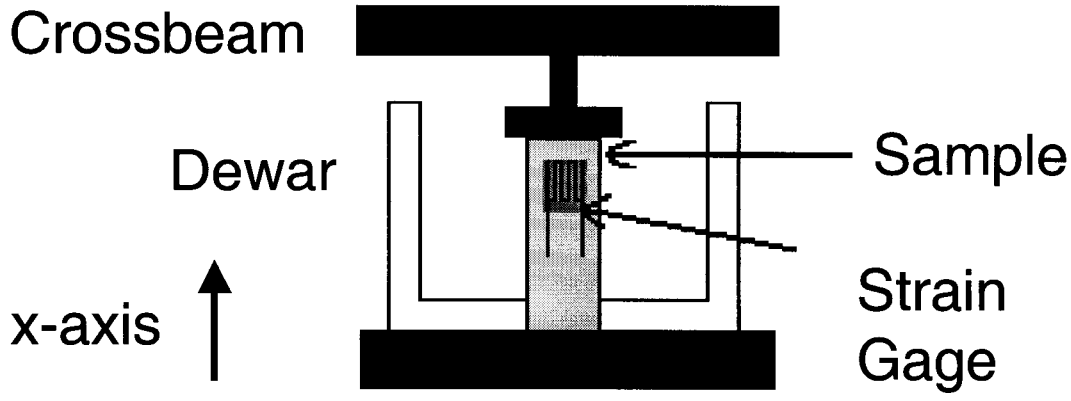

Figure 4.1: Schematic of the magnetomechanical damping measurement device.

magnetostrictive performance and thermal expansion properties. The samples were placed in a styrofoam dewar filled with liquid nitrogen, but the bottom of the sample was in contact with a rigid base plate on the lower crosshead. This configuration allowed for measurements of the x-axis compression at room and liquid nitrogen temperatures. Since magnetoelastic effects are temperature dependent [5], we confirmed uniformity of surface temperatures of the samples during measurements with a silicon diode thermometer. The specimen was then subjected to compressive stress in the x-direction of the sample from the crosshead as controlled by a computer. Stresses varied from 0 to 25-50 MPa with the crosshead motion was 0.5 mm/min, resulting in a cycling frequency of roughly 0.02-0.08 Hz. In some tests, we used stress ranges with minima above zero in order to ascertain the damping properties in various stress regimes. Because of the fact that the applied stress of deformation along the z-axis of each of our samples resulted in thicknesses of around 4

mm and because relatively large (~1 mm) grain sizes made measurements with small strain gauges unreliable, measurements of strain in the samples' z-axes were not possible.

For each sample, measurements were repeated at 300 K. This allows for a comparison of damping effects and Young's modulus of polycrystalline TbDy at ferromagnetic and paramagnetic temperatures. Since there is no ferromagnetism at this temperature, we expected little stress-strain hysteresis from these measurements.

4.3 Results of Polycrystalline TbDy Damping

Cyclic stress-strain curves measured on a sample of polycrystalline $Tb_{0.76}Dy_{0.24}$ of commercial purity (sample 76c1) are shown in Figure 4.2. The effects of magnetoelastic coupling during the 77 K measurements are clearly evident from the pronounced hysteresis in the stress-strain curve. The same measurements at 300 K show no measurable hysteresis. The local strains provided by domain reorientation occur at stresses much lower than required by work against the interatomic force constants, which are expected to be approximately the same at 77 K as at 300 K. Also, the elastic modulus of the sample softens considerably for measurements at 77 K. Corresponding measurements performed on a high purity sample of polycrystalline $Tb_{0.76}Dy_{0.24}$ (sample 76h1) are shown in Figure 4.3. In each case, intermediate cyclic stress-strain curves were also measured at 77 K, providing the minor loops shown in Figures 4.2 and 4.3. The widths of the hysteresis loops in the stress-strain curves are reduced at higher applied stresses for both samples, indicating saturation of magnetization and a resulting decrease in damping.

Table 4.1 contains a summary of the measurements of average elastic moduli and

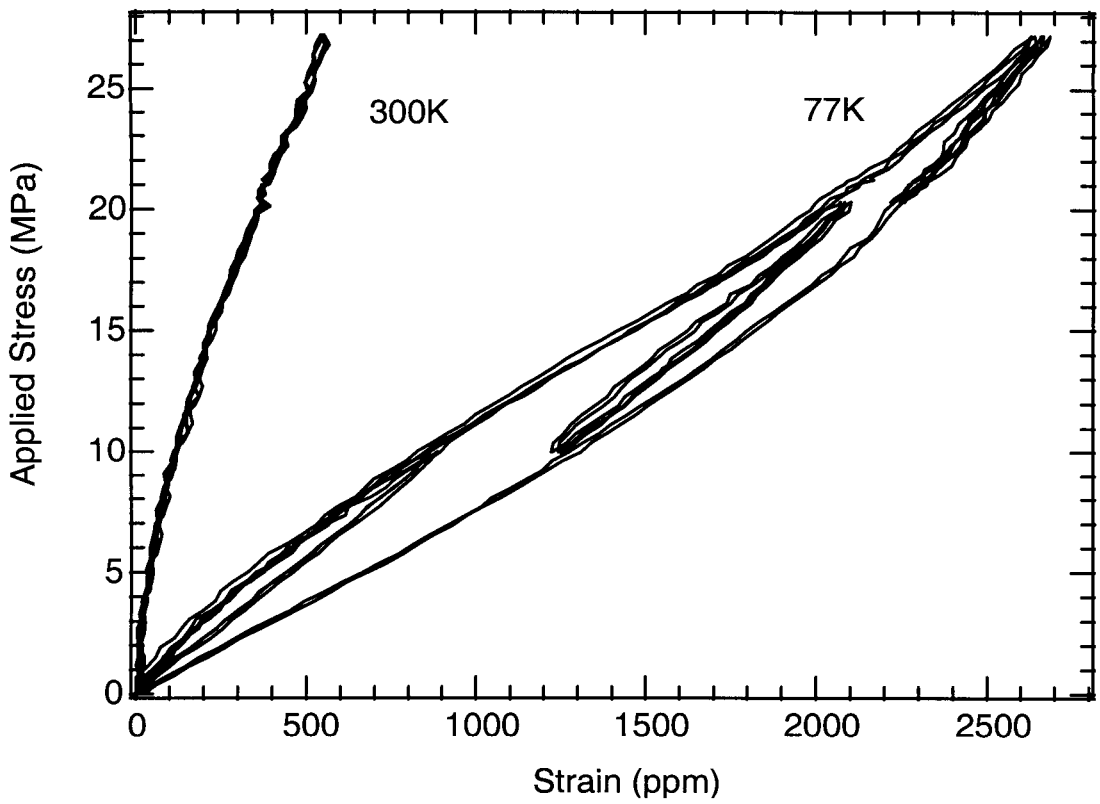

Figure 4.2: Stress-strain curves for polycrystalline $Tb_{0.76}Dy_{0.24}$, commercial purity (sample 76c1).

energy dissipations of polycrystalline $Tb_{0.76}Dy_{0.24}$ alloys. The elastic moduli listed are defined as the average slope of the stress-strain curve within the applied stress range indicated. The measurements of elastic modulus at 300K results are in reasonable agreement with the values of 59.1 GPa reported for $Tb_{0.76}Dy_{0.24}$ [6]. At 77 K we observed up to fivefold and threefold reductions in Young's moduli for the commercial purity and high purity samples, respectively. The 77 K elastic moduli of 17.2 and 10.0 GPa for the high-purity and commercial purity polycrystalline $Tb_{0.76}Dy_{0.24}$ are consistent with 15 GPa elastic modulus measurements of $Tb_{0.6}Dy_{0.4}$ hot rolled sheets [2]. It is interesting that the stress-strain

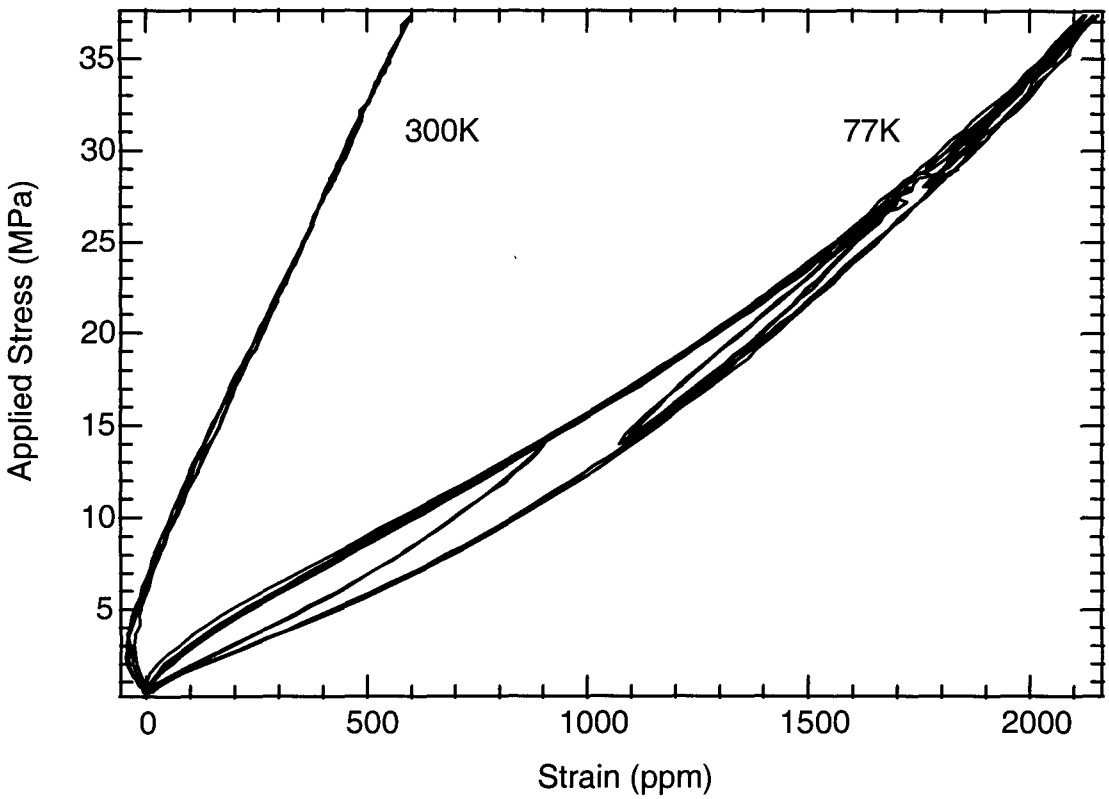

Figure 4.3: Stress-strain curves for polycrystalline $Tb_{0.76}Dy_{0.24}$, high purity (sample 76h1).

curves at 77 K begin to curve upwards at stresses of approximately 25 MPa. For minor loops, elastic moduli are consistently higher at higher ranges of applied stresses. This is due to domain reorientation occurring primarily at lower stresses, so at higher stresses the domain reorientation provides a decreasing amount of additional strain. We do not expect to measure elastic moduli at 77 K equal those seen at 300 K because plastic deformation begins to occur at stresses of approximately 40-50 MPa.

The stress-strain curves of Figures 4.2 and 4.3 show mechanical hysteresis loops that indicate substantial energy dissipation. The fractional dissipation figures in Table 4.2 is calculated as the ratio of the area of the hysteresis loop to the mean area under the loading

Sample and Applied Stress	Modulus at 77 K (GPa)	Modulus at 300 K (GPa)
76c1 - 0-27 MPa	10.0	49.6
76c1 - 0-10 MPa	10.5	
76c1 - 10-20 MPa	13.3	
76c1 - 20-27 MPa	16.7	
76h1 - 0-36 MPa	17.2	57.2
76h1 - 0-14 MPa	15.6	
76h1 - 14-28 MPa	21.5	
76h1 - 28-36 MPa	23.0	

Table 4.1: Elastic modulus of polycrystalline $Tb_{0.76}Dy_{0.24}$ over various applied stresses.

and unloading curves. The energy lost is the product of the fractional dissipation with total potential energy stored within sample. The fraction of mechanical energy dissipated in the material is as large as 22.6% for the commercial purity sample. This is sufficient to make polycrystalline Tb-Dy an interesting material for the damping of mechanical vibrations at cryogenic temperatures.

Sample and Applied Stress	Fractional Dissipation
76c1 - 0-27 MPa	18.2%
76c1 - 0-10 MPa	22.6%
76c1 - 10-20 MPa	16.5%
76h1 - 0-36 MPa	13.8%
76h1 - 0-14 MPa	16.7%
76h1 - 14-28 MPa	12.9%

Table 4.2: Mechanical damping of polycrystalline $Tb_{0.76}Dy_{0.24}$.

The minor loops of mechanical hysteresis showed decreasing damping effects for higher applied stresses. Again, greater domain realignments at low strains are responsible for their larger mechanical dissipation properties. This effect has been observed previously with other magnetoelastic materials also measured for several cycles at restricted ranges of applied stress [1, 7]. Also, the small total area of the minor hysteresis loops compared

to larger loops over the same stress range indicate that the magnetic domain orientations depend strongly on the mechanical history of the sample. Hence, the reorientations corresponding to the minor hysteresis loops are more easily reversed than those that take place over a wider range of strain.

The clear differences in magnetoelastic damping and magnetostrictive properties of commercial purity and high purity samples of TbDy alloys are difficult to explain with our limited texture data. Impurities such as oxygen can potentially act as impediments to grain growth and could therefore alter the texture of deformed commercial purity TbDy alloys. An examination of grain sizes by optical metallography revealed grains ranging from a tenth of a millimeter to more than one millimeter in length for both 76h1 and 76c1, but no clear differences in grain size between the samples were observed. More sophisticated grain orientation analysis measurements have the potential to provide a better understanding of grain size relationships to texture and composition of TbDy alloys, and are discussed in Chapter 5.

4.4 Measurement of damping by stress-induced magnetization of a solenoid

A direct way to measure magnetomechanical effects of applied stresses is to measure a magnetostrictive sample's induced magnetization. By measuring the current in a solenoid around a magnetostrictive sample subject to an applied load, the change in magnetic field and therefore change in magnetization of the sample can be determined. Unfortunately, external electronic and mechanical noise from the Instron load frame prevented

the use of this technique in the above experiments.

In order to gain some insight into how a polycrystalline TbDy sample magnetizes under a load, we measured the current of a 3900-turn solenoid around TbDy sample 60c1 of rectangular dimensions 32.4 × 5.1 × 2.9 mm. The sample and solenoid were placed in the same dewar used in the Instron tests, and the sample rested on an aluminum plate while immersed in LN_2. The sample was struck with a wooden beam to induce a shock wave. A typical result is shown in Figure 4.4, with the signal voltage (proportional to current) plotted versus time. Since the applied force is not well controlled in this experiment, the data is of limited use but some aspects of the sample's magnetoelastic behavior are nonetheless apparent. Because the sample is being magnetized by an impact force, we assume that the solenoid's signal is being diminished by the dissipation of vibrations within the sample. The signal's period of approximately 35-40 ms correspond to sound velocities of 1.6-1.8 km/s, similar to measured velocities in polycrystalline TbDy of 1.7 km/s and 2.9 km/s for ultrasonic shear and longitudinal waves respectively. This strongly suggests that each peak in the signal represents one cycle of vibration of the sample. Hence, a rough estimation of the sample's damping characteristics can be made from this data.

By fitting the peaks of the oscillations to decaying exponential curves as in Figure 4.4, we notice a decay in the amplitude of the signal peaks of ~23% of per cycle. This compares closely to our measured low stress quasistatic damping capacities of TbDy alloys shown in Table 4.1. While this result is preliminary, the high frequency damping capacity of TbDy is nonetheless apparent. More sophisticated measurements of dynamic stress-induced magnetization of TbDy alloys may reveal further high frequency damping properties and

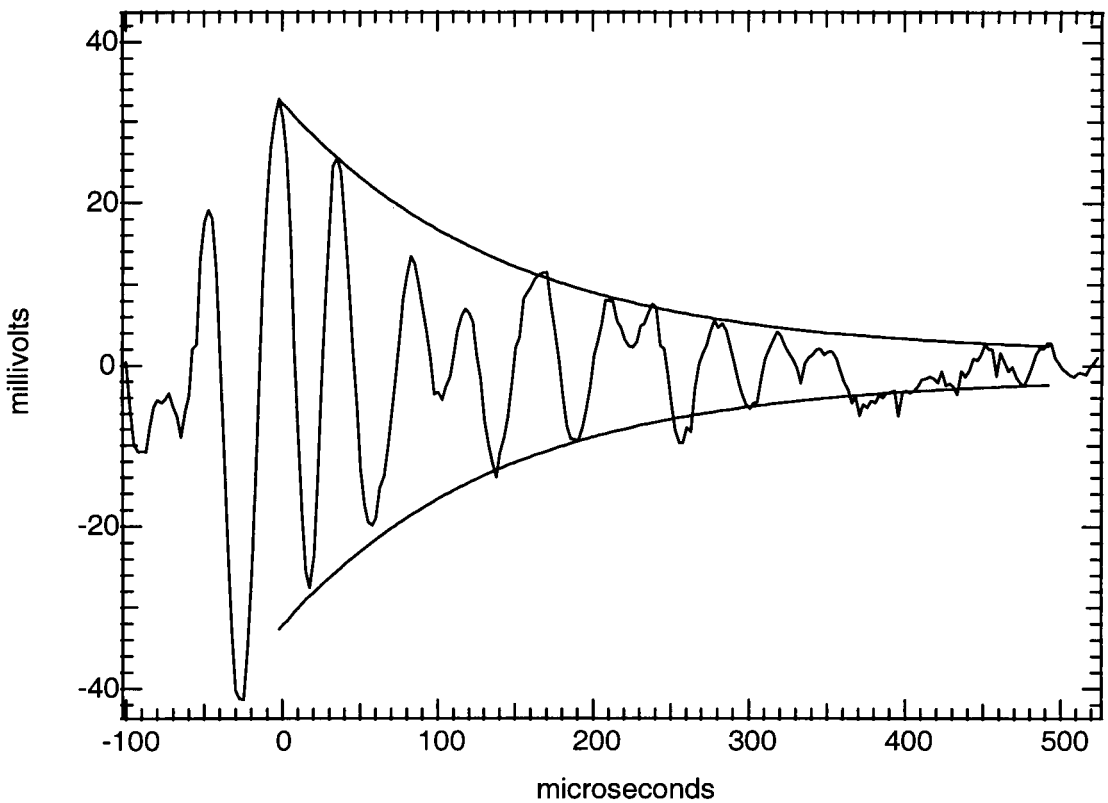

Figure 4.4: Magnetoelastic damping signal from a polycrystalline TbDy sample. The exponential curves are fitted to the peaks of the oscillating signal.

their relation to grain orientation and microstructure.

4.5 Analysis

The mechanical damping properties of TbDy alloys are inexorably linked to their magnetostriction properties. A first order analysis of this relation utilizes the model by Cochardt introduced in Chapter 1 [8, 9]. In this model, we can use measured length magnetostriction λ, elastic modulus E, and strain ε to obtain the fraction of energy dissipated:

$$\Delta U = \frac{k\lambda E}{\varepsilon_c^2}\varepsilon^3 \tag{4.1}$$

ε_c is the critical strain where no further dissipation takes place. ΔU is per unit volume, so the result is multiplied by the volume of each sample in order to compare to experiment. Unfortunately, ε_c is difficult to determine in the case of our samples because plastic deformation starts to occur at stresses of 40 MPa. Below this stress, the elastic modulus is not close to room temperature values and mechanical hysteresis is still evident. Nonetheless, mechanical hysteresis becomes small above 30 MPa as can be seen in Figure 3, and nearly disappears by 40 MPa, so we choose ε_c to be the strain corresponding to 50 MPa of stress (approximately 4200 ppm for 76c1, 3000 ppm for 76h1) as a likely lower bound. Also, following Laddha and Van Aken [9], we take k, a function of hysteresis curve shape, to be unity. The results are calculated energy dissipations which are compared to our measurements.

While typical measured dissipations per cycle are 2×10^{-3} J for full stress-strain cycles of both of our samples, the model predicts dissipations about an order of magnitude too large. The underestimated ε_c may account for some of the discrepancy. Also, since the model neglects the effects of grain boundaries and other microstructures of polycrystalline TbDy as impediments to domain realignment, it is not surprising that we obtain an overestimate of mechanical dissipation. Since grains of differing orientations will have varying directions of hard magnetic anisotropy, domains will be forced to jump over resulting energy barriers and therefore require higher stresses to dissipate energy, an effect neglected here.

A number of models for magnetomechanical damping have been developed to accurately account for magnetic domain jumping between easy axes of anisotropy. In one

such model, the multiple hard axes of cubic Terfenol-D are seen as barriers to domain reorientation and the primary source of magnetomechanical loss [1, 7]. However, since applied stresses will not produce magnetization jumps by 180°, this model is not useful for hexagonal TbDy or any other uniaxial material. A more general model by Smith and Birchak [10] assumes energy loss from domain rotation when applied stress exceeds a local stress barrier σ_{loc}:

$$\Delta U_{\text{loc}} = k\lambda\sigma_{\text{loc}},\ \sigma \geq \sigma_{\text{loc}} \tag{4.2}$$

While this model shows promise for analysis of damping in polycrystalline TbDy, it presents formidable barriers in the calculation of local stress barriers σ_{loc}. Further discussion of this approach will be presented in Chapter 5.

Bibliography

[1] J. P. Teter, K. B. Hathaway and A. E. Clark, J. Appl. Phys. **79**, 6213 (1996).

[2] A. E. Clark, M. Wun-Fogle, J. B. Restoff and J. F. Lindberg, IEEE Trans Magn. **29**, 3511 (1993).

[3] E. A. Brandes, ed. *Smithells Metals Reference Book* (Butterworths, Bodmin UK, 1983) p. 15-5.

[4] S. B. Palmer, E. W. Lee and M. N. Islam, Proc. Roy. Soc. **A338**, 341 (1974).

[5] J. J. Rhyne and A. E. Clark, J. Appl. Phys. **38**, 1379 (1967).

[6] N. V. Kadobnova and A. M. Bratovskii, *Handbook of Physical Quantities* (CRC Press, Boca Raton FL, 1997).

[7] K. B. Hathaway, A. E. Clark and J. P. Teter, Metal. and Mater. Trans. **26A**, 2797 (1995).

[8] A. W. Cochardt, Trans. ASME, J. Appl. Mech. **75**, A196 (1953).

[9] S. Laddha and D. C. Van Aken, Metal. Mater. Trans. **26A**, 957 (1995).

[10] G. W. Smith and J. R. Birchak, J. Appl. Phys. **40**, 5174 (1969).

Chapter 5

Future Research

From the preceding work, it is clear that textured polycrystalline alloys of TbDy possess magnetostrictive strain and magnetomechanical damping properties which are large enough to be of technological interest. We found that grain orientations and interactions play a large role in the magnetoelastic properties of TbDy alloys. In this chapter, future work needed to better characterize the magnetoelastic properties of TbDy is outlined.

5.1 Grain orientation measurements

In Chapter 2 the results of thermal expansion were used to describe the grain texture of TbDy. The asymmetry of texture in the plane of deformation was clear in measurements of expansion through magnetic phase transitions. Also, the thermal expansion anisotropy of polycrystalline versus single crystal TbDy samples was used to correlate increased texture to larger magnetostrictive strokes and larger damping capacities. A more complete measure of grain orientations will allow for more rigorous analysis of these effects.

By measuring the ultrasonic wave velocities through TbDy samples, grain orientations can be established as an expansion of modified spherical harmonics [1,2]:

$$w(\cos\theta,\psi,\phi)=\sum_{l=0}^{\infty}\sum_{m=-l}^{l}\sum_{n=-l}^{l}W_{lmn}Z_{lmn}(\cos\theta)\exp^{-im\psi}\exp^{-in\phi} \tag{5.1}$$

with $w(\cos\theta,\psi,\phi)$ the probability density of finding a grain at an Euler angle (θ,ψ,ϕ). $Z_{lmn}(\cos\theta)$ are generalized associated Legendre functions and W_{lmn} are the measured orientation distribution functions. From such information, pole diagrams of texture can be obtained and a more thorough analysis of bulk texture of the effects of bulk texture on the magnetoelastic properties of TbDy alloys can be performed.

The standard technique of x-ray diffraction pole figure analysis is possible, but our own work shows this to be difficult for two reasons: the necessarily large grains of TbDy samples requiring the use of averaging over many samples, and the ability to measure only surface texture. Since at 30keV x-rays penetrate Tb and Dy only 100 microns, bulk grain texture measurements of the interior of TbDy alloys with this method are problematic. Unfortunately, neutron diffraction measurements, also commonly used to characterize texture of alloys, are frustrated by a large neutron absorption cross-section of Dy nuclei. Another technique involving backscattered electrons from a scanning electron microscope beam has been shown to provide surface texture information for cubic polycrystals; further development of analysis software will allow for texture determination of hexagonal materials such as TbDy in the future.

5.2 Domain interaction with grain boundaries

Magnetization is caused by the motion of domain walls as domains form, realign and grow. Such movement is affected by changes in magnetocrystalline anisotropy across grain boundaries, especially with a material as highly anisotropic in one axis as TbDy. An analysis of the influence of microstructure on domain wall boundary motion and its effect on magnetoelastic dissipation in TbDy would aid in understanding texture dependent magnetoelastic behavior. The model developed by Smith and Birchak [3] discussed in Chapter 4 could be applied to TbDy alloys so as to gain insight into the effects of domain jumping between easy directions of magnetization of adjacent grains. Such jumping must overcome a potentially large energy barrier if nearby grains have misaligned c-axes. This rapid domain movement induces energy loss by a distribution of local stress barriers $N(\sigma_{\text{loc}})$: [4]

$$\Delta U = \int_0^{\sigma} \Delta U_{\text{loc}} N(\sigma_{\text{loc}})\, \mathrm{d}\sigma_{\text{loc}} \tag{5.2}$$

The local stress barriers in TbDy will be governed by local stresses between grains and relative magnetocrystalline anisotropies. Therefore, a detailed knowledge of grain alignment is necessary to perform such an analysis.

Experimentally, rapid movement of domains could be observed during magnetomechanical damping by measuring rapid changes in magnetization through induction of a pickup coil. Both the speed and magnitude of the domain fluctuations will affect the induced current of the coil. Such an investigation would be a more sophisticated version of the dynamic damping tests described in Chapter 4. The use of a model of domain jumping induced damping in conjunction with induction measurements could prove useful in under-

standing the role of domain realignment in magnetoelastic damping of TbDy polycrystals.

The basic foundation of the Smith-Birchak model can be further refined by measuring the local dissipative effects of grain boundaries. A technique called magnetic force microscopy [5] allows for a magnetized cantilever's motion to map the surface magnetoelastic dissipations of a magnetoelastic material. The induced domain wall oscillations are modeled as a damped harmonic oscillator and reveal the effects of small-scale structures on domain motion and resulting dissipations [6]. Such information would be valuable in assessing the microstructural influences of various deformation and annealing procedures on the damping properties of TbDy polycrystalline alloys.

Bibliography

[1] C. M. Sayers, J. Phys. D **15,** 2157 (1982).

[2] M. Hirao, K. Aoki and H. Fukuoka. J. Acoust. Soc. Am. **81**, 1434 (1987).

[3] G. W. Smith and J. R. Birchak, J. Appl. Phys. **40**, 5174 (1969).

[4] S. Laddha and D. C. Van Aken, Metal. Mater. Trans. **26A**, 957 (1995).

[5] P. Grutter, Y. Liu, P. LeBlanc and U. During, Appl. Phys. Lett. **71**, 279 (1997).

[6] Y. Liu and P. Grutter, J. Appl. Phys. **83**, 5922 (1998).